High Order Approximation of Advection-Diffusion Problems on Polygonal Meshes

Todd Arbogast

Center for Subsurface Modeling,

Oden Institute for Computational Engineering and Sciences

and Department of Mathematics

The University of Texas at Austin

- Maicon R. Correa, University of Campinas, Brazil
- Chieh-Sen Huang, National Sun Yat-sen Univ., Taiwan

- Danielle King, Raytheon corporation, USA
- Zhen Tao, Google corporation
- Chenyu Tian, University of Texas at Austin, USA
- Chuning Wang, University of Minnesota, USA
- Xikai Zhao, Schlumberger corporation, USA

This work was supported by the U.S. National Science Foundation and the Taiwan Ministry of Science and Technology

Outline

I. Introduction and Motivation

II. Conforming Finite Element Approximations

Extend the theory of serendipity and mixed finite elements on rectangles to polygons

1. Direct serendipity finite elements for approx. of scalar functions
2. Direct mixed elements for approximation of vector functions
3. Approximation properties
4. Application to tracer transport

III. Discontinuous Finite Volume WENO Approximations

Develop an accurate and flexible reconstruction for multi-dimensional problems

1. Stencil polynomial approximations
2. New multilevel weighted essentially non-oscillatory (ML-WENO) reconstruction
3. Some numerical results
4. Preliminary application to two-phase flow (Richards equation)

IV. Summary and Conclusions

I. Introduction and Motivation

Advection-Diffusion-Reaction Equations

$$\boxed{u_t + \nabla \cdot [f(u) - D(u)\nabla u] = q(u)}$$

Models in science and engineering often embody conservation laws for

1. Advection, $u_t + \nabla \cdot f(u) = 0$
   - conservative transport of a substance
   - mathematically hyperbolic
2. Diffusion, $u_t - \nabla \cdot D(u)\nabla u = 0$
   - spreading or mixing of a substance to the average of its surroundings
   - mathematically parabolic (or elliptic)
3. Reactions, $u_t = q(u)$ [Omit for this talk]
   - substances transform to other substances or phases
   - mathematically an ordinary differential equation

These are systems of advection-diffusion-reaction equations.

- The equations may be advection dominated
- The diffusion may degenerate to zero
- The solution to the equations can develop steep fronts or shocks

$$\boxed{u_t + \nabla \cdot f(u) = 0}$$

- Mass conservative
- Linear transport in 1D is simple translation

$$u_t + a u_x = 0, \; u(x,0) = u_0(x) \quad \Longrightarrow \quad u(x,t) = u_0(x - at)$$

A discontinuity in u_0 propagates as a contact discontinuity.

- Nonlinear transport in 1D has variable speed

$$u_t + f'(u)\, u_x = 0, \; u(x,0) = u_0(x)$$

If $f(u)$ grows with u, a shock discontinuity can form.

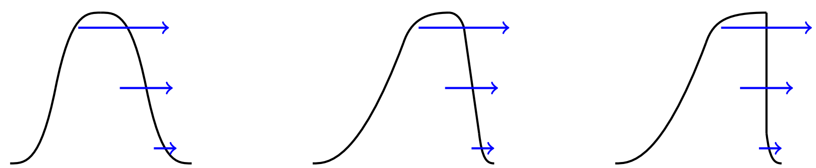

- Solutions do not become smoother in time (the solution operator is *not* compact), but solutions are total variation diminishing

$$\mathrm{TV}(u)(t) = \int |u_x(x,t)|\, dx \le \mathrm{TV}(u_0) = \int |u_0'(x)|\, dx$$

The solution does not oscillate.

- Hyperbolic scaling: Space and time scale as $t \sim x$

$$u(x,t) = U(\xi(x,t)) \quad \Longrightarrow \quad u_t = U'\xi_t \sim u_x = U'\xi_x \quad \Longrightarrow \quad dt \sim dx$$

$$\boxed{u_t - \nabla \cdot [D(u)\nabla u] = 0}$$

- Mass conservative
- Solutions smooth in time (the solution operator is compact on Sobolev spaces)

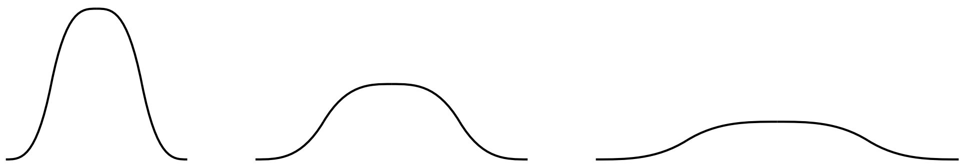

- Solutions are continuous. Initial discontinuities disappear immediately.
- The maximum principle: u is the average of nearby values. The solution does not oscillate.
- Parabolic scaling: Space and time scale as $t \sim x^2$

$$u(x,t) = U(\xi(x,t)) \quad \Longrightarrow \quad u_t = U'\xi_t \sim u_{xx} = U'\xi_{xx} + U''(\xi_x)^2$$
$$\Longrightarrow \quad dt \sim dx^2$$

Solve the physical problem **accurately**

1. Conserve mass locally.
2. Support discontinuous solutions, to handle shocks or steep fronts.
3. Satisfy the maximum principle, or at least non-oscillatory solutions.

Compute **efficiently**

4. Use high order methods in space. More efficient use of the DoFs.
5. Use high order, implicit methods in time. Improves stability.
6. Use a minimal number of degrees of freedom (DoFs). Reduces memory bandwidth.

Handle medium **heterogeneity** (specific to porous media)

7. General computational meshes. Follow rock strata and allow local refinement.


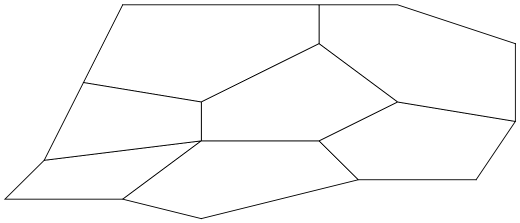
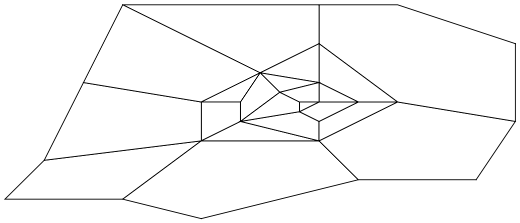

8. Maximize the mesh resolution. Better resolve the heterogeneity in the permeability and porosity.

Main Difficulty: These objectives are in opposition to each other!

II. Conforming Finite Element Approximations

Challenges:

- Not many conforming finite elements on polygons are available.
- We want finite elements with the minimal number of DoFs.

Minimal DoF Elements on Rectangles

Related by de Rham complex. (Arnold, Falk & Winther 2006)

$$\mathbb{R} \hookrightarrow H^1(E_4) \xrightarrow{\text{curl}} H(\text{div}, E_4)) \xrightarrow{\text{div}} L^2(E_4) \longrightarrow 0$$

$$\mathbb{R} \hookrightarrow \mathcal{S}_{r+1}(E_4) \xrightarrow{\text{curl}} \text{BDM}_r(E_4) \xrightarrow{\text{div}} \mathbb{P}_{r-1}(E_4) \longrightarrow 0$$

Serendipity finite elements. $\mathcal{S}_r$ on rectangle E_4

- $\mathcal{S}_r = \mathbb{P}_r(E_4) \oplus \text{span}\{x^r y, xy^r\}$
- H^1-conforming
- Approximate scalars to $\mathcal{O}(h^{r+1})$

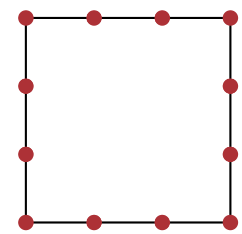

$\mathcal{S}_3 \supset \mathbb{P}_3$
($\mathcal{S}_3 \neq \mathbb{P}_{3,3}$)

BDM mixed finite elements. BDM_r on rectangle E_4

- $\text{BDM}_r = \mathbb{P}_r^2 \oplus \text{span}\{\text{curl}(x^r y), \text{curl}(xy^r)\}$
- $H(\text{div})$-conforming
- Approximate vectors to $\mathcal{O}(h^{r+1})$

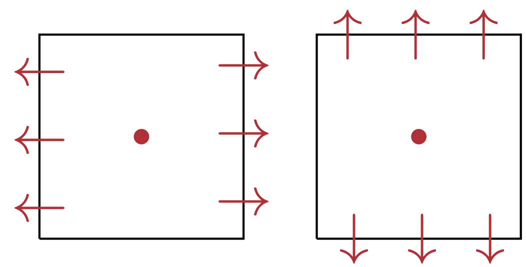

v_1 v_2

$\text{BDM}_2 \supset \mathbb{P}_2^2$

Finite elements for the divergence $\mathbb{P}_r$ on rectangle E_4

- $\mathbb{P}_r(E_4)$
- L^2-conforming (no continuity)
- Approximate scalars to $\mathcal{O}(h^{r+1})$

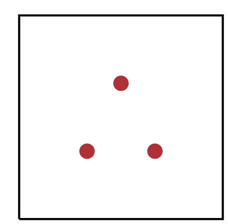

$\mathbb{P}_1$

Extend the theory of serendipity and mixed finite elements on rectangles to polygons

Challenge. Quadrilaterals are *not* affine equivalent to squares.

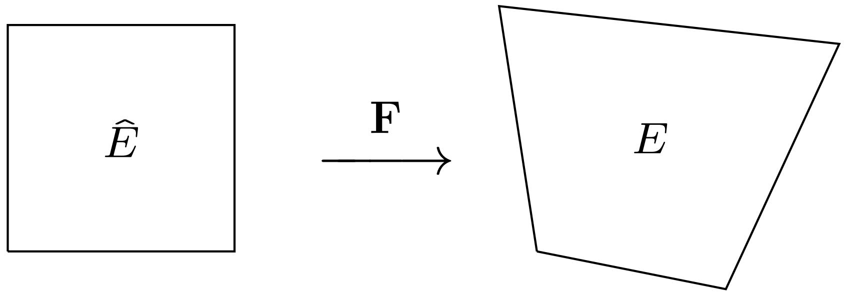

The map $\mathbf{F} : \widehat{E} \to E$ is bilinear, so we lose accuracy in the approximation.

Solution. We define direct finite element spaces that

- include polynomials $\mathbb{P}_r$ *directly* in the space (for approximation)
- use minimal number of DoFs subject to Sobolev space conformity

Strategy. For a convex polygon E_N with N sides,

1. first define direct serendipity elements $\mathcal{DS}_r(E_N)$
2. then use de Rham theory to define direct mixed elements $\mathbf{V}_r(E_N)$

1. Direct Serendipity Finite Elements $\mathcal{DS}_r(E_N)$ for Approximation of Scalars

Require $\mathcal{DS}_r(E_N) \supset \mathbb{P}_r(\mathbb{R}^2)$

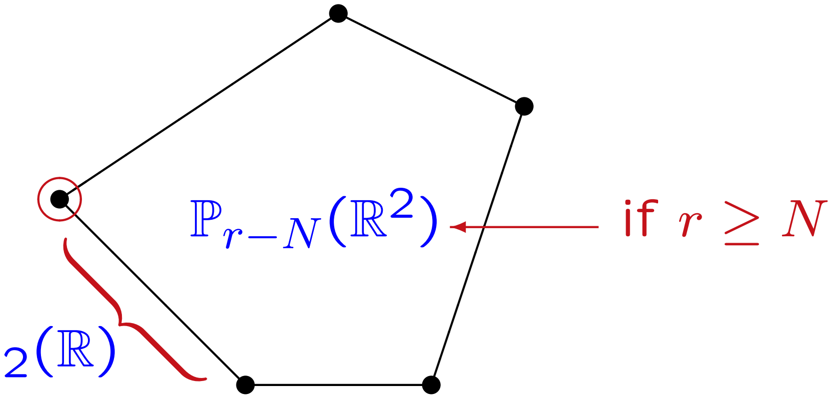

if $r \geq 2 \longrightarrow \mathbb{P}_{r-2}(\mathbb{R})$

DoFs required for H^1-Conformity ($N \geq 3$, $r \geq 1$)

Object	Object Count	DoFs per Object	Total DoFs
vertex	N	1	N
interior edge	N	$\dim \mathbb{P}_{r-2}(\mathbb{R})$	$N(r-1)$
interior cell	1	$\dim \mathbb{P}_{r-N}(\mathbb{R}^2)$	$\underbrace{\frac{1}{2}(r-N+2)(r-N+1)}_{\text{provided } r \geq N-2}$

Minimal DoFs.

$$\dim \mathcal{DS}_r(E_n) = \dim \mathbb{P}_r(E) + \begin{cases} \frac{1}{2}N(N-3), & r \geq N-2 \\ Nr - \frac{1}{2}(r+2)(r+1), & r < N-2 \end{cases}$$

Require a Supplemental Space $\mathbb{S}_r^{\mathcal{DS}}(E_N)$

The DoF count implies

$$\boxed{\mathcal{DS}_r(E_N) = \mathbb{P}_r(E_N) \oplus \mathbb{S}_r^{\mathcal{DS}}(E_N)} \qquad \big(\text{so } \mathbb{P}_r(E_N) \cap \mathbb{S}_r^{\mathcal{DS}}(E_N) = \{0\}\big)$$

where

$$\dim \mathbb{S}_r^{\mathcal{DS}}(E_N) = \begin{cases} \frac{1}{2}N(N-3), & r \geq N-2 \\ Nr - \frac{1}{2}(r+2)(r+1) < \frac{1}{2}N(N-3), & r < N-2 \end{cases}$$

Case $r \geq N-2$. For each of the N edges, there are $N-3$ nonadjacent edges. That is, the number of nonadjacent edge pairs is

$$\frac{1}{2}N(N-3) = \dim \mathbb{S}_r^{\mathcal{DS}}(E_N)$$

Supplemental basis functions arise from nonadjacent pairs of edges!

Case $r < N-2$: Counterintuitive observation. Case $r \geq N-2$ is easier! Cannot build higher order spaces from $r = 1$ (barycentric coordinates). We will define $\mathcal{DS}_r(E_N) \subset \mathbb{S}_{N-2}^{\mathcal{DS}}(E_N)$.

Use CCW Ordering
(and mod N as needed).

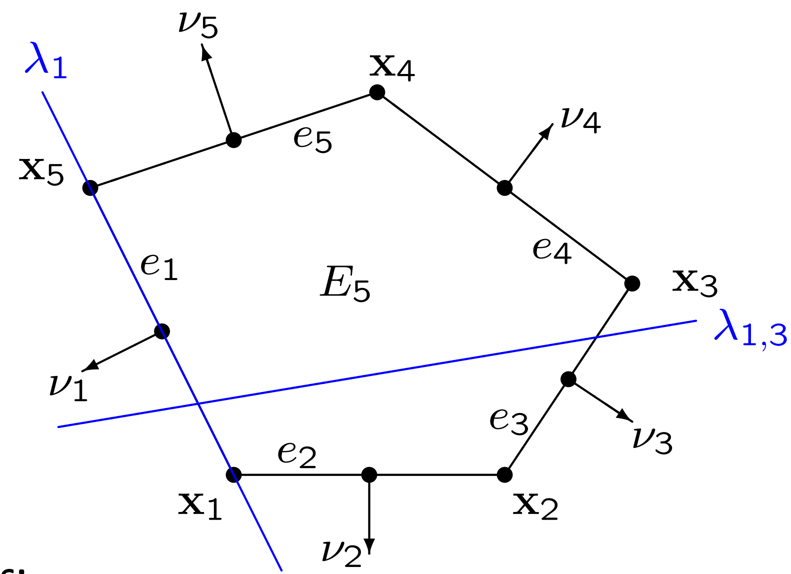

Linear polynomial λ_i for edge e_i. Define

$$\lambda_i(\mathbf{x}) = -(\mathbf{x} - \mathbf{x}_i) \cdot \nu_i \quad \propto$$

distance of $\mathbf{x}$ to the line through edge e_i

$$\implies \lambda_i\Big|_{e_i} = 0 \quad \text{(zero line contains } e_i\text{)}$$

$$\lambda_i > 0 \quad \text{on the interior of } E_N$$

Not barycentric coordinates!

Linear polynomial $\lambda_{i,j}$ for edges e_i and e_j. Choose *any* linear polynomial $\lambda_{i,j}$ with zero line joining e_i and e_j. (Connect the midpoints?)

For e_i and e_j *not* adjacent and $i < j$ (mod N), take any $R_{i,j}(\mathbf{x})$ such that

$$\begin{cases} R_{i,j}(\mathbf{x})|_{e_i} = -1 \\ R_{i,j}(\mathbf{x})|_{e_j} = 1 \end{cases}$$

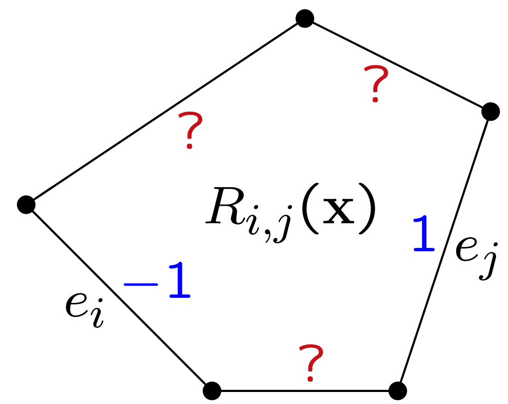

Examples.

- A rational function (but can be hard to integrate)

$$R_{i,j}(\mathbf{x}) = \frac{\lambda_i(\mathbf{x}) - \lambda_j(\mathbf{x})}{\lambda_i(\mathbf{x}) + \lambda_j(\mathbf{x})}$$

- A piecewise continuous function so that quadrature rules are exact.

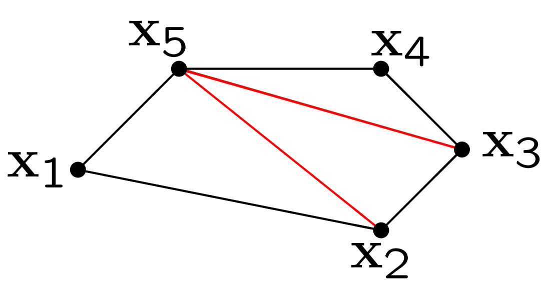

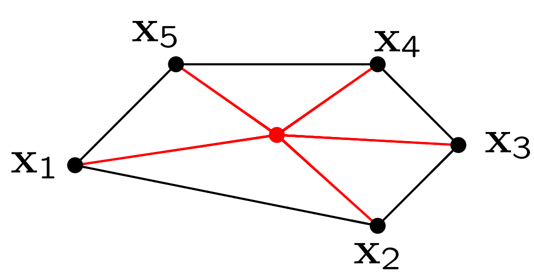

Theorem. The finite element

$$\mathcal{DS}_r(E_N) = \mathbb{P}_r(E_N) \oplus \mathbb{S}_r^{\mathcal{DS}}(E_N)$$
$$\mathbb{S}_r^{\mathcal{DS}}(E_N) = \{\varphi_{i,j} : i,j = 1,\dots,N,\ i,j \text{ nonadjacent}\}$$

$$\varphi_{i,j} = \underbrace{\underbrace{\Big(\prod_{m\neq i,j} \lambda_m\Big)}_{\substack{=0 \text{ except}\\ \text{on edges } i,j}} \quad \underbrace{\lambda_{i,j}^{r-N+2}}_{\substack{\text{variation}\\ \text{on edges } i,j}}}_{\text{polynomial of degree } r} \quad \underbrace{R_{i,j}}_{\substack{\text{opposite signs}\\ \text{on edges } i,j}}$$

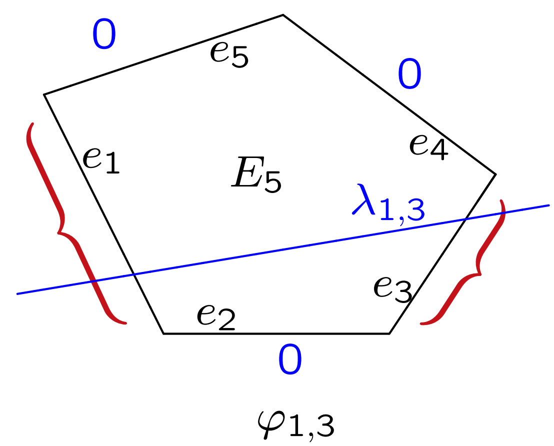

is well defined (i.e., unisolvent with nodal DoFs).

Moreover, it has the minimal number of DoFs needed

- to contain $\mathbb{P}_r$
- for H^1 conformity

Examples of Basis Functions

Edge node for $\mathcal{DS}_3$ on a pentagon

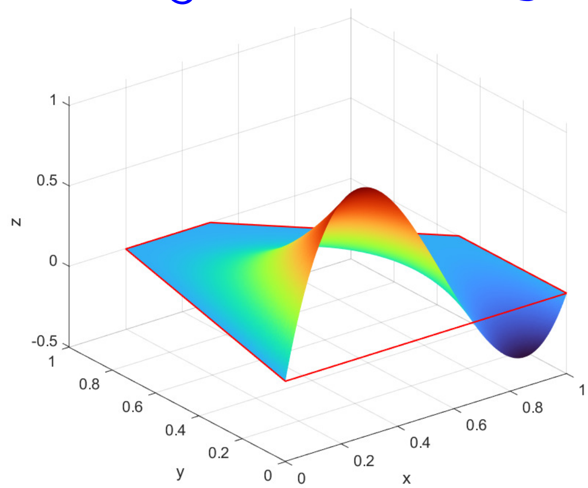

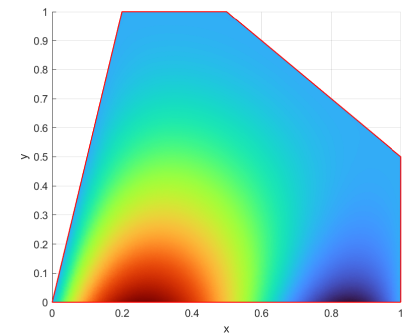

Vertex node for $\mathcal{DS}_3$ on a pentagon

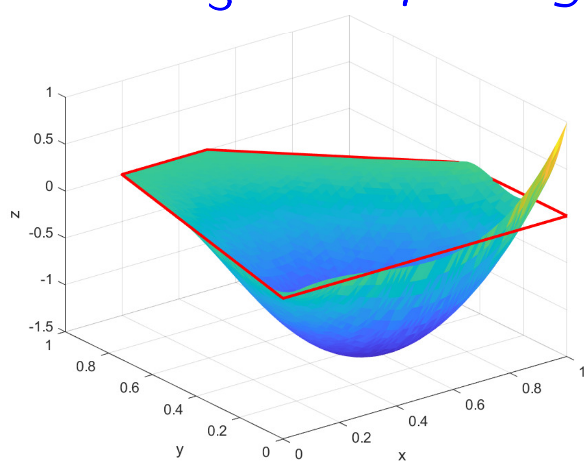

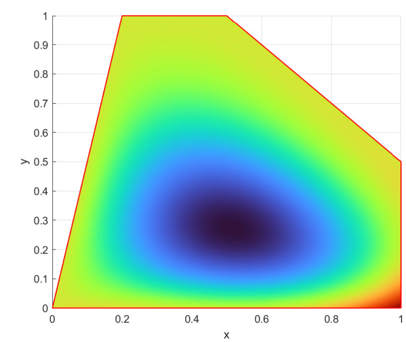

Lack of symmetry makes it difficult to define supplemental functions!

Examples. $\mathcal{DS}_r(E_5)$

$r = 1 \implies$ 2 supplemental functions

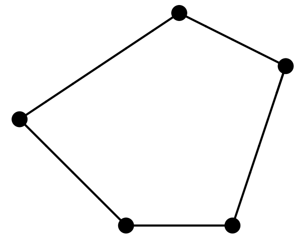

$r = 2 \implies$ 4 supplemental functions

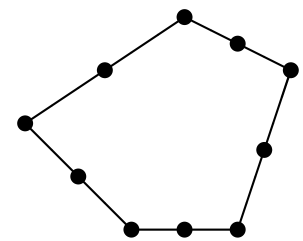

Definition. Take $\mathcal{DS}_r(E_N) \subset \mathcal{DS}_{N-2}(E_N)$, i.e.,

$$\boxed{\mathcal{DS}_r(E_N) = \left\{\varphi \in \mathcal{DS}_{N-2}(E_N) : \varphi|_{e_i} \in \mathbb{P}_r(e_i) \text{ for all edges } e_i \text{ of } E_N\right\}}$$

Theorem. The finite element $\mathcal{DS}_r(E_N)$ is well defined (i.e., unisolvent with nodal DoFs) when $r < N-2$. Moreover,

$$\mathcal{DS}_r(E_N) = \mathbb{P}_r(E_N) \oplus \mathbb{S}_r^{\mathcal{DS}}(E_N) \ \subset \ \mathcal{DS}_{N-2}(E_N)$$

for some supplemental space of minimal dimension needed for H^1-conformity.

Basis Functions of $\mathcal{DS}_1(E_5)$

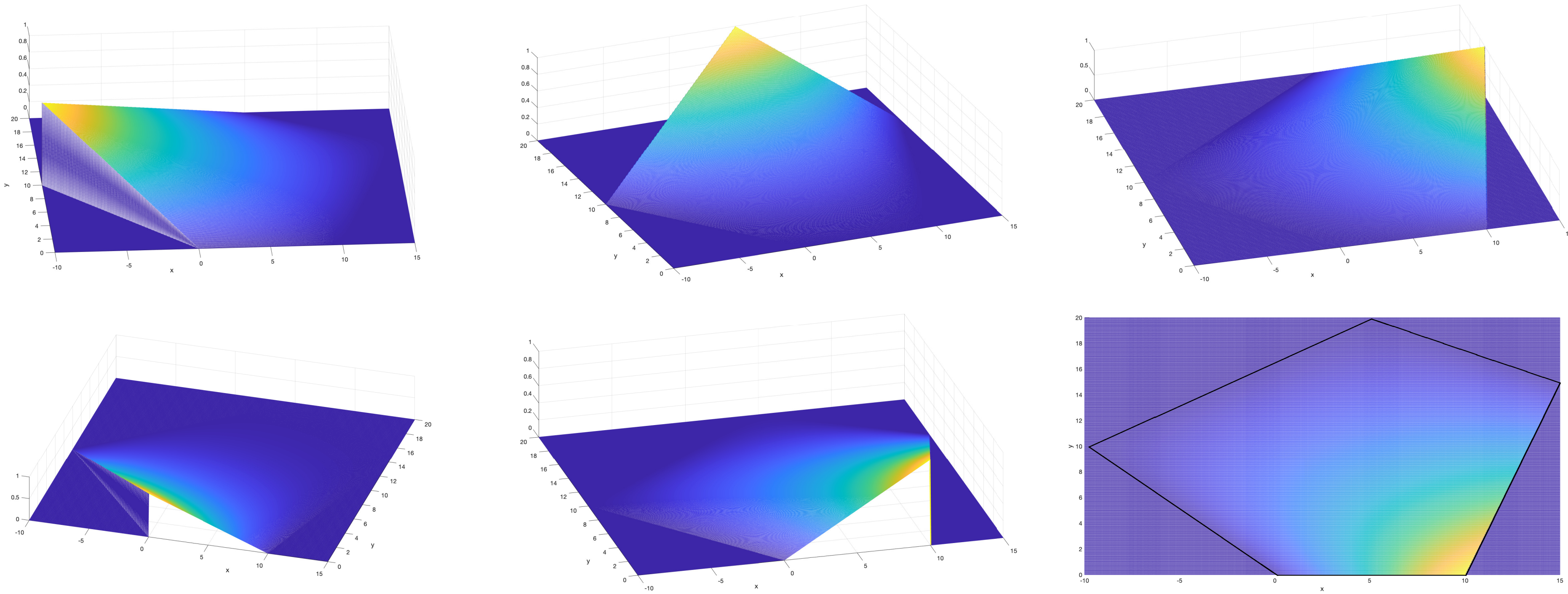

Remark. These appear to be barycentric coordinates (but we do not prove they are nonnegative).

2. Direct Mixed Elements $\mathbf{V}_r^s(E_N)$ for Approximation of Vectors

The de Rham complex of interest

$$\boxed{\mathbb{R} \hookrightarrow H^1 \xrightarrow{\text{curl}} H(\text{div}) \xrightarrow{\text{div}} L^2 \longrightarrow 0}$$

- The curl (or rot) of a scalar function is

$$\text{curl}\,\phi = \left(\frac{\partial\phi}{\partial x_2}, -\frac{\partial\phi}{\partial x_1}\right)$$

- The image of one linear map is the kernel of the next

We have the decompositions

$$\underbrace{\mathbb{R} \xhookrightarrow{i} i(\mathbb{R}) \oplus \left(H^1/\mathbb{R}\right)}_{= H^1} \xrightarrow{\text{curl}} \underbrace{\text{curl}\left(H^1/\mathbb{R}\right) \oplus \mathbf{G}}_{= H(\text{div})} \xrightarrow{\text{div}} \underbrace{\text{div}\,\mathbf{G}}_{= L^2} \xrightarrow{0} 0$$

$$\text{curl}\, i(\mathbb{R}) = 0 \qquad\qquad \text{curl}\,\text{div} = 0$$

Thus

$$\text{div} : \mathbf{G} \xrightarrow{\text{1 to 1, onto}} L^2 \qquad \Longrightarrow \qquad \mathbf{G} = \text{div}^{-1} L^2$$

Helmholtz decomposition

$$H(\text{div}) = \text{curl}\left(H^1/\mathbb{R}\right) \oplus \mathbf{G}, \qquad \mathbf{G} = \{\nabla\varphi : \varphi \in H^1\}$$

$$\mathbb{R} \hookrightarrow H^1 \xrightarrow{\text{curl}} H(\text{div}) \xrightarrow{\text{div}} L^2 \longrightarrow 0$$

Finite Element Exterior Calculus (Arnold, Falk & Winther 2006)

$$\mathbb{R} \hookrightarrow \mathcal{DS}_{r+1}(E_N) \xrightarrow{\text{curl}} \mathbf{V}_r^s(E_N) \xrightarrow{\text{div}} \mathbb{P}_s(E_N) \longrightarrow 0$$

Fact: $\nabla\cdot : \mathbf{x}\mathbb{P}_s \to \mathbb{P}_s$ is one-to-one and onto

1. *Reduced H(div)-approximating direct finite elements* $(s = r-1, r \geq 1)$

$$\begin{aligned}
\mathbf{V}_r^{r-1}(E_N) &= \text{curl}\,\mathcal{DS}_{r+1}(E_N) \oplus \mathbf{x}\mathbb{P}_{r-1} \qquad (\mathcal{DS}_{r+1} = \mathbb{P}_{r+1} \oplus \mathbb{S}_{r+1}^{\mathcal{DS}}(E_N)) \\
&= \text{curl}\,\mathbb{P}_{r+1}(E_N) \oplus \text{curl}\,\mathbb{S}_{r+1}^{\mathcal{DS}}(E_N) \oplus \mathbf{x}\mathbb{P}_{r-1} \\
&= \mathbb{P}_r^2(E_N) \oplus \mathbb{S}_r^{\mathbf{V}}(E_N) \qquad (\mathbb{P}_r^2 = \text{curl}\,\mathbb{P}_{r+1} \oplus \mathbf{x}\mathbb{P}_{r-1})
\end{aligned}$$

The supplemental (vector valued) functions are

$$\mathbb{S}_r^{\mathbf{V}}(E_N) = \text{curl}\,\mathbb{S}_{r+1}^{\mathcal{DS}}(E_N)$$

2. *Full H(div)-approximating direct finite elements* $(s = r \geq 0)$

$$\begin{aligned}
\mathbf{V}_r^r(E_N) &= \text{curl}\,\mathcal{DS}_{r+1}(E_N) \oplus \mathbf{x}\mathbb{P}_r \\
&= \text{curl}\,\mathbb{P}_{r+1}(E_N) \oplus \mathbf{x}\mathbb{P}_r \oplus \text{curl}\,\mathbb{S}_{r+1}^{\mathcal{DS}}(E_N) \\
&= \mathbb{P}_r^2(E_N) \oplus \mathbf{x}\underbrace{\tilde{\mathbb{P}}_r}_{\text{homogeneous polynomials}} \oplus \mathbb{S}_r^{\mathbf{V}}(E_N) \qquad (\mathbb{P}_r^2 = \text{curl}\,\mathbb{P}_{r+1} \oplus \mathbf{x}\mathbb{P}_{r-1})
\end{aligned}$$

1. Edge DoFs: $\displaystyle\int_{e_i} \boldsymbol{\psi} \cdot \nu_i \, p \, d\sigma \quad \forall p \in \mathbb{P}_r(e_i),\ i = 1, 2, \dots, N$

   Control normal components

2. Divergence DoFs: $\displaystyle\int_{E_N} \boldsymbol{\psi} \cdot \nabla q \, dx \quad \forall q \in \mathbb{P}_s(E_N),\ q$ not constant

   Control divergence

3. Curl DoFs: $\displaystyle\int_{E_N} \boldsymbol{\psi} \cdot \mathbf{v} \, dx \quad \forall \mathbf{v} \in \mathbb{B}_r^{\mathbf{V}}(E_N) = \operatorname{curl} \mathbb{B}_{r+1}(E_N)$

   Control the curl (if $r \geq N-1$)

$$\mathbb{B}_{r+1}(E_N) = \lambda_1 \lambda_2 \dots \lambda_N \, \mathbb{P}_{r-N+1}(E_N)$$

Theorem. Let $r = 0, 1, \dots$ and $s = r$ or $s = r - 1 \geq 0$.

The finite element $\mathbf{V}_r^s(E_N)$ is well defined (i.e., unisolvent).

Moreover, it has the minimal number of DoFs needed so that

- $\mathbf{V}_r^s(E_N) \supset \mathbb{P}_r^2$
- $\mathbf{V}_r^s(E_N)$ is $H(\text{div})$ conforming
- $\nabla \cdot \mathbf{V}_r^s(E_N) = \mathbb{P}_s$

3. Approximation Properties

Let $\mathcal{T}_h$ be a uniformly shape regular partition of Ω into convex polygons.

Interpolation operators. We can define operators

- Scott-Zhang interpolation $\mathcal{I}_h^r$ into $\mathcal{DS}_r$ (cf. Scott & Zhang 1990)
- Raviart-Thomas projection $\pi_h^{r,s}$ into $\mathbf{V}_r^s$ (cf. Raviart & Thomas 1977)
- L^2 projection $\mathcal{P}_{W_s}$ into $W_h = \nabla \cdot \mathbf{V}_r^s$

Theorem. For scalar p and $m = 0, 1$,

$$\inf_{w_h \in \mathcal{DS}_r(\Omega)} \|p - w_h\|_{H^m(\Omega)} \le \|p - \mathcal{I}_h^r p\|_{H^m(\Omega)} \le C\, h^{r+1-m}\, \|v\|_{H^{r+1}(\Omega)}$$

Theorem. For vector $\mathbf{u}$ and scalar p, with $s = r-1, r$ $(s \ge 0)$,

$$\begin{aligned}
\|\mathbf{u} - \pi_h^{r,s}\mathbf{u}\|_{L^2} &\le C\, \|\mathbf{u}\|_{H^{r+1}}\, h^{r+1} \\
\|\nabla \cdot (\mathbf{u} - \pi_h^{r,s}\mathbf{u})\|_{L^2} &\le C\, \|\nabla \cdot \mathbf{u}\|_{H^{s+1}}\, h^{s+1} \\
\|p - \mathcal{P}_{W_s} p\|_{L^2} &\le C\, \|p\|_{H^{s+1}}\, h^{s+1}
\end{aligned}$$

Moreover, the discrete inf-sup condition holds for some $\gamma > 0$:

$$\sup_{\mathbf{v}_h \in \mathbf{V}_r^s} \frac{(w_h, \nabla \cdot \mathbf{v}_h)}{\|\mathbf{v}_h\|_{H(\mathrm{div})}} \ge \gamma\, \|w_h\|_{L^2}, \quad \forall w_h \in W_s$$

Convergence tests: Use a manufactured solution

$$p(x,y) = \sin(\pi x)\sin(\pi y) \quad \text{solving} \quad -\Delta p = f, \quad 0 < x < 1,\ 0 < y < 1$$

Convergence for $\mathbb{P}_{r,r}$, $\mathcal{S}_r$, and $\mathcal{DS}_r$ on Trapezoids—1

L^2-errors and convergence rates on trapezoidal meshes

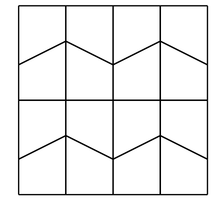

n	$r=2$ error	$r=2$ rate	$r=3$ error	$r=3$ rate	$r=4$ error	$r=4$ rate	$r=5$ error	$r=5$ rate
	mapped $\mathbb{P}_{r,r}$, dim $=\mathcal{O}(r^2)$							
8	3.329e-04	2.99	9.740e-06	3.99	2.382e-07	4.99	5.076e-09	5.99
12	9.888e-05	2.99	1.928e-06	3.99	3.142e-08	5.00	4.462e-10	6.00
16	4.176e-05	3.00	6.107e-07	4.00	7.459e-09	5.00	7.946e-11	6.00
24	1.238e-05	3.00	1.207e-07	4.00	9.827e-10	5.00	6.979e-12	6.00
		$\mathcal{O}(h^3)$		$\mathcal{O}(h^4)$		$\mathcal{O}(h^5)$		$\mathcal{O}(h^6)$
	mapped $\mathcal{S}_r$, dim $=\mathcal{O}(r^2/2)$							
8	5.714e-04	2.92	4.844e-04	2.89	2.612e-05	3.72	2.005e-06	4.13
12	1.731e-04	2.94	1.482e-04	2.92	6.084e-06	3.59	3.884e-07	4.05
16	7.409e-05	2.95	6.383e-05	2.93	2.265e-06	3.43	1.234e-07	3.99
24	2.254e-05	2.94	1.963e-05	2.91	5.984e-07	3.28	2.516e-08	3.92
48	3.127e-06	2.82	2.825e-06	2.76	6.875e-08	3.09	1.850e-09	3.71
64	1.440e-06	2.70	1.332e-06	2.61	2.862e-08	3.05	6.644e-10	3.56
		$\mathcal{O}(h^?)$		$\mathcal{O}(h^?)$		$\mathcal{O}(h^?)$		$\mathcal{O}(h^?)$
	direct $\mathcal{DS}_r$, dim $=\mathcal{O}(r^2/2)$							
8	3.492e-04	3.00	3.897e-05	4.07	2.187e-06	5.00	8.896e-08	5.96
12	1.036e-04	3.00	7.457e-06	4.08	2.889e-07	4.99	7.870e-09	5.98
16	4.373e-05	3.00	2.313e-06	4.07	6.868e-08	4.99	1.404e-09	5.99
24	1.296e-05	3.00	4.469e-07	4.05	9.058e-09	5.00	1.235e-10	6.00
		$\mathcal{O}(h^3)$		$\mathcal{O}(h^4)$		$\mathcal{O}(h^5)$		$\mathcal{O}(h^6)$

Convergence for $\mathbb{P}_{r,r}$, $\mathcal{S}_r$, and $\mathcal{DS}_r$ on Trapezoids—2

H^1-seminorm errors & convergence rates on trapezoidal meshes

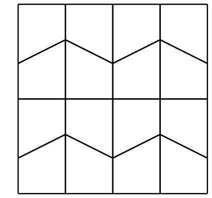

	$r=2$		$r=3$		$r=4$		$r=5$	
n	error	rate	error	rate	error	rate	error	rate
$\mathbb{P}_{r,r}$, dim $= \mathcal{O}(r^2)$								
8	1.734e-02	2.00	7.206e-04	2.99	2.310e-05	3.99	6.083e-07	4.99
12	7.710e-03	2.00	2.139e-04	3.00	4.570e-06	4.00	8.021e-08	5.00
16	4.337e-03	2.00	9.027e-05	3.00	1.447e-06	4.00	1.904e-08	5.00
24	1.928e-03	2.00	2.676e-05	3.00	2.859e-07	4.00	2.509e-09	5.00
		$\mathcal{O}(h^2)$		$\mathcal{O}(h^3)$		$\mathcal{O}(h^4)$		$\mathcal{O}(h^5)$
$\mathcal{S}_r$, dim $= \mathcal{O}(r^2/2)$								
8	2.413e-02	1.94	1.834e-02	1.90	1.818e-03	2.65	1.537e-04	3.18
12	1.105e-02	1.93	8.572e-03	1.88	6.582e-04	2.51	4.483e-05	3.04
16	6.432e-03	1.88	5.091e-03	1.81	3.345e-04	2.35	1.945e-05	2.90
24	3.104e-03	1.80	2.560e-03	1.70	1.360e-04	2.22	6.370e-06	2.75
48	1.043e-03	1.50	9.409e-04	1.37	3.190e-05	2.07	1.140e-06	2.41
64	7.097e-04	1.34	6.602e-04	1.23	1.776e-05	2.03	5.953e-07	2.26
		$\mathcal{O}(h^?)$		$\mathcal{O}(h^?)$		$\mathcal{O}(h^?)$		$\mathcal{O}(h^?)$
$\mathcal{DS}_r$, dim $= \mathcal{O}(r^2/2)$								
8	1.836e-02	2.01	2.517e-03	3.02	1.625e-04	3.99	7.384e-06	4.99
12	8.143e-03	2.00	7.400e-04	3.02	3.216e-05	4.00	9.757e-07	4.99
16	4.577e-03	2.00	3.109e-04	3.01	1.018e-05	4.00	2.318e-07	5.00
24	2.033e-03	2.00	9.170e-05	3.01	2.012e-06	4.00	3.056e-08	5.00
		$\mathcal{O}(h^2)$		$\mathcal{O}(h^3)$		$\mathcal{O}(h^4)$		$\mathcal{O}(h^5)$

Convergence Study for $\mathcal{DS}_r$ Polygons

Meshes. PolyMesher (Talischi et al. 2012) using $n \times n$ random initial seeds. $N = 6$ mostly, but some $N = 4, 5$

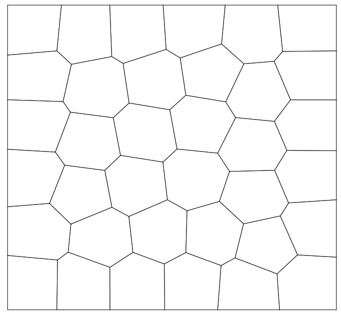

$6 \times 6 = 36$ elements

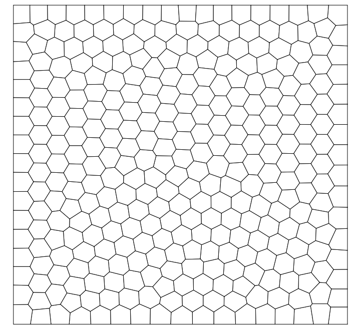

$18 \times 18 = 324$ elements

Errors and convergence rates for direct serendipity spaces

n	$r = 2$ error	rate	$r = 3$ error	rate	$r = 4$ error	rate	$r = 5$ error	rate
				L^2-norm				
10	2.160e-04	3.45	8.859e-06	4.34	3.467e-07	5.69	1.133e-08	6.97
14	7.329e-05	3.16	2.175e-06	4.11	5.644e-08	5.31	1.202e-09	6.57
18	3.454e-05	3.30	8.172e-07	4.29	1.544e-08	5.68	3.080e-10	5.97
22	1.881e-05	3.26	3.605e-07	4.39	5.476e-09	5.56	8.151e-11	7.13
		$\mathcal{O}(h^3)$		$\mathcal{O}(h^4)$		$\mathcal{O}(h^5)$		$\mathcal{O}(h^6)$
				H^1-seminorm				
10	3.561e-03	2.32	1.933e-04	3.13	8.530e-06	4.55	3.103e-07	5.73
14	1.683e-03	2.19	6.724e-05	3.09	1.973e-06	4.29	4.625e-08	5.57
18	1.018e-03	2.20	3.194e-05	3.26	6.992e-07	4.55	1.553e-08	4.78
22	6.762e-04	2.19	1.743e-05	3.25	3.035e-07	4.48	4.995e-09	6.09
		$\mathcal{O}(h^2)$		$\mathcal{O}(h^3)$		$\mathcal{O}(h^4)$		$\mathcal{O}(h^5)$

Convergence Study for $\mathbb{V}_r^{r-1}$ on Polygons

Errors and convergence rates for
reduced $H(\text{div})$-approximation direct mixed spaces

n	$\|\|p-p_h\|\|$ error	rate	$\|\mathbf{u}-\mathbf{u}_h\|$ error	rate	$\|\nabla\cdot(\mathbf{u}-\mathbf{u}_h)\|$ error	rate
			$r=1$			
10	1.290e-01	1.24	1.770e-02	2.29	1.260e-01	1.15
14	9.109e-02	1.02	8.997e-03	1.98	9.001e-02	0.98
18	7.039e-02	1.13	5.429e-03	2.21	6.988e-02	1.11
22	5.734e-02	1.10	3.619e-03	2.18	5.707e-02	1.09
		$\mathcal{O}(h)$		$\mathcal{O}(h^2)$		$\mathcal{O}(h)$
			$r=2$			
10	8.635e-03	2.23	5.013e-04	3.24	8.634e-03	2.23
14	4.308e-03	2.04	1.785e-04	3.02	4.308e-03	2.03
18	2.616e-03	2.19	8.487e-05	3.26	2.616e-03	2.19
22	1.719e-03	2.25	4.649e-05	3.23	1.719e-03	2.25
		$\mathcal{O}(h^2)$		$\mathcal{O}(h^3)$		$\mathcal{O}(h^2)$
			$r=3$			
10	3.878e-04	3.38	1.992e-05	4.37	3.878e-04	3.38
14	1.384e-04	3.02	5.102e-06	3.99	1.384e-04	3.02
18	6.516e-05	3.30	1.889e-06	4.36	6.516e-05	3.30
22	3.514e-05	3.31	8.363e-07	4.37	3.514e-05	3.31
		$\mathcal{O}(h^3)$		$\mathcal{O}(h^4)$		$\mathcal{O}(h^3)$

Convergence Study for $\mathbf{V}_r^r$ on Polygons

Errors and convergence rates for full $H(\mathrm{div})$-approximation

n	$\|\|p - p_h\|\|$ error	rate	$\|\mathbf{u} - \mathbf{u}_h\|$ error	rate	$\|\nabla \cdot (\mathbf{u} - \mathbf{u}_h)\|$ error	rate
			$r = 0$			
10	1.282e-01	1.20	5.915e-02	1.59	1.260e-01	1.15
14	9.089e-02	1.01	3.577e-02	1.47	9.001e-02	0.98
18	7.030e-02	1.13	2.701e-02	1.23	6.988e-02	1.11
22	5.730e-02	1.10	2.005e-02	1.60	5.707e-02	1.09
		$\mathcal{O}(h)$		$\mathcal{O}(h)$		$\mathcal{O}(h)$
			$r = 1$			
10	8.635e-03	2.23	1.892e-03	2.67	8.634e-03	2.23
14	4.308e-03	2.04	8.562e-04	2.32	4.308e-03	2.03
18	2.616e-03	2.19	4.903e-04	2.44	2.616e-03	2.19
22	1.719e-03	2.25	3.142e-04	2.39	1.719e-03	2.25
		$\mathcal{O}(h^2)$		$\mathcal{O}(h^2)$		$\mathcal{O}(h^2)$
			$r = 2$			
10	3.881e-04	3.38	6.546e-05	3.69	3.881e-04	3.38
14	1.384e-04	3.02	1.945e-05	3.55	1.384e-04	3.02
18	6.516e-05	3.30	8.982e-06	3.39	6.516e-05	3.30
22	3.514e-05	3.31	4.448e-06	3.77	3.514e-05	3.31
		$\mathcal{O}(h^3)$		$\mathcal{O}(h^3)$		$\mathcal{O}(h^3)$
			$r = 3$			
10	1.299e-05	4.59	2.473e-06	5.15	1.299e-05	4.59
14	3.270e-06	4.04	5.434e-07	4.44	3.270e-06	4.04
18	1.188e-06	4.44	2.220e-07	3.92	1.188e-06	4.44
22	5.259e-07	4.37	1.021e-07	4.17	5.259e-07	4.37
		$\mathcal{O}(h^4)$		$\mathcal{O}(h^4)$		$\mathcal{O}(h^4)$

Consider mesh sequences with $n = 6, 10, 14, 18, 22$ and $r = 5$ of mostly

- $N = 3$, triangles (regular and random)
- $N = 4$, squares, regular quadrilaterals, random quadrilaterals
- $N = 6$, hexagons (regular and random)

Log-log plot of errors versus half the number of DoFs

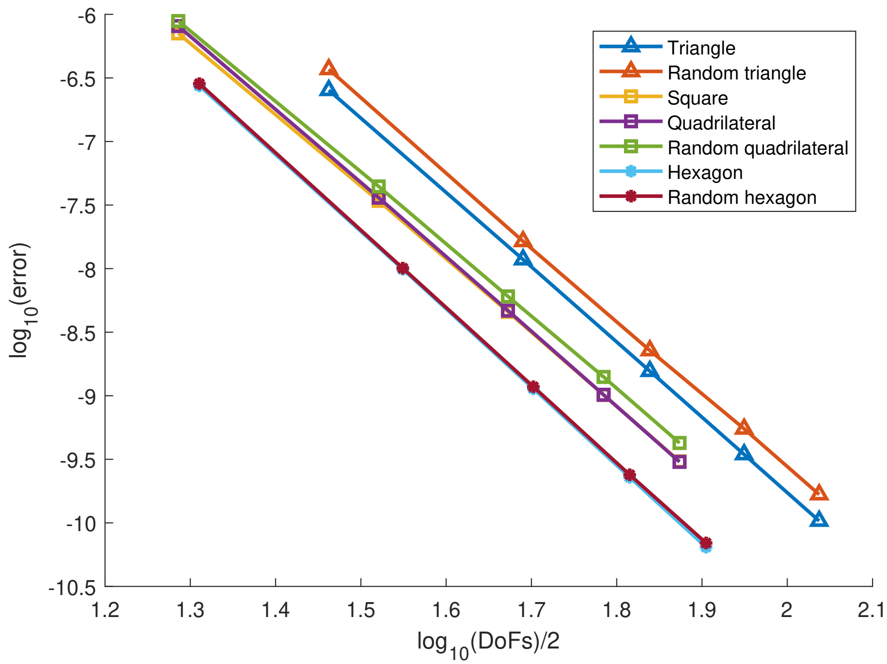

L^2-norm

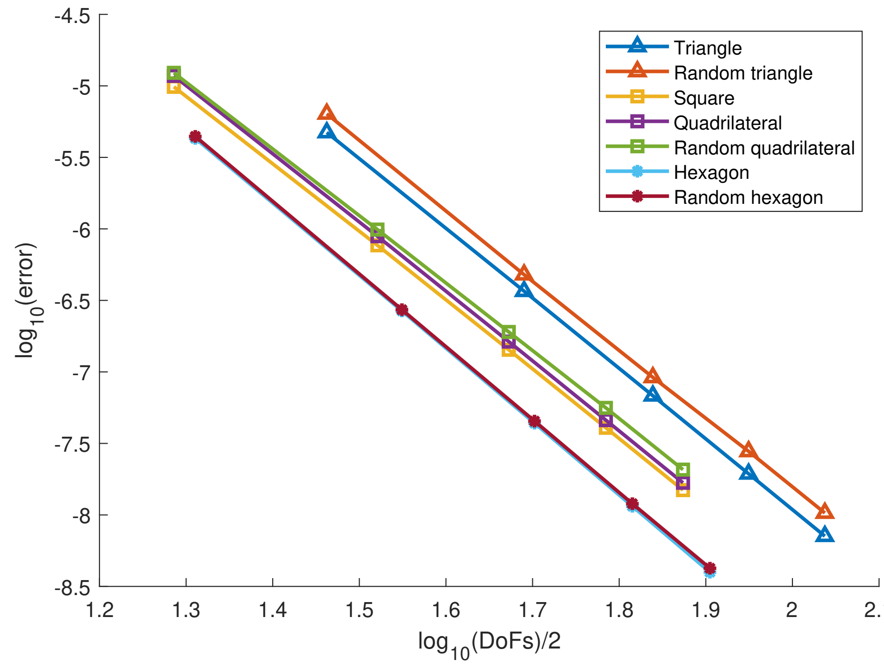

H^1-seminorm

Remark. We see for greater accuracy for meshes with more sides!

4. Application to Tracer Transport

Governing equations.

Flow: $\begin{cases} \mathbf{u} = -\nabla p \\ \nabla \cdot \mathbf{u} = 0 \end{cases}$ Direct Mixed FE $\mathbf{V}_1^1$

Transport: $\dfrac{\partial c}{\partial t} + \nabla \cdot (c\mathbf{u} - \nabla c) = 0$ Enriched Galerkan (EG)

DG_0 enriched with $\mathcal{DS}_2$ (Sun & Liu 2009)

plus Entropy Viscosity (Guermond, Pasquetti & Popov 2011)

Flow solution.

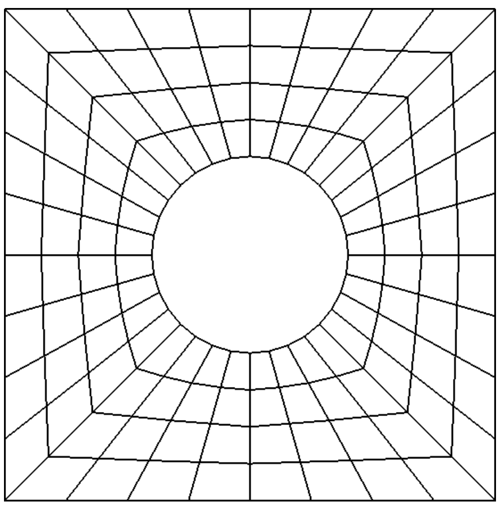

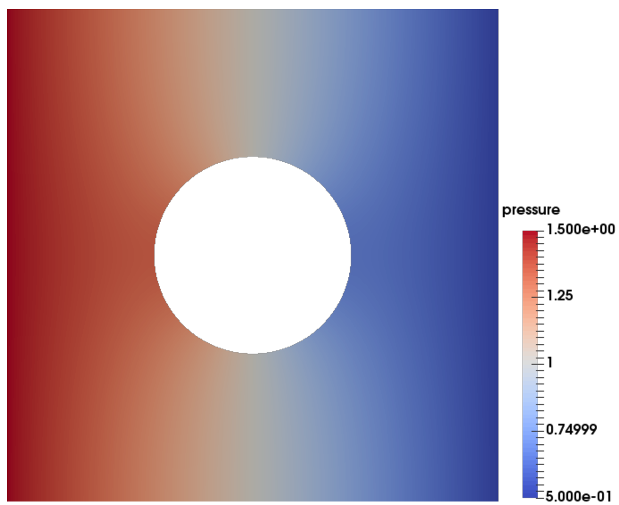

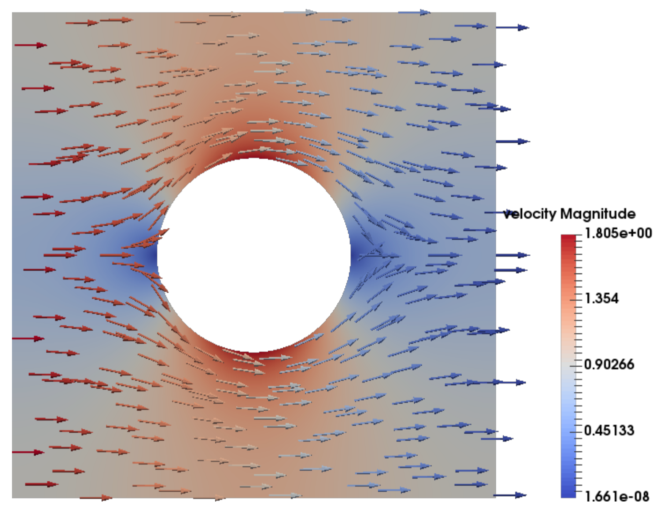

Coarse mesh

128 elements

Pressure Velocity

8192 elements

Concentration. (8192 elements, $\Delta t = 0.1 h_{\text{min}}$)

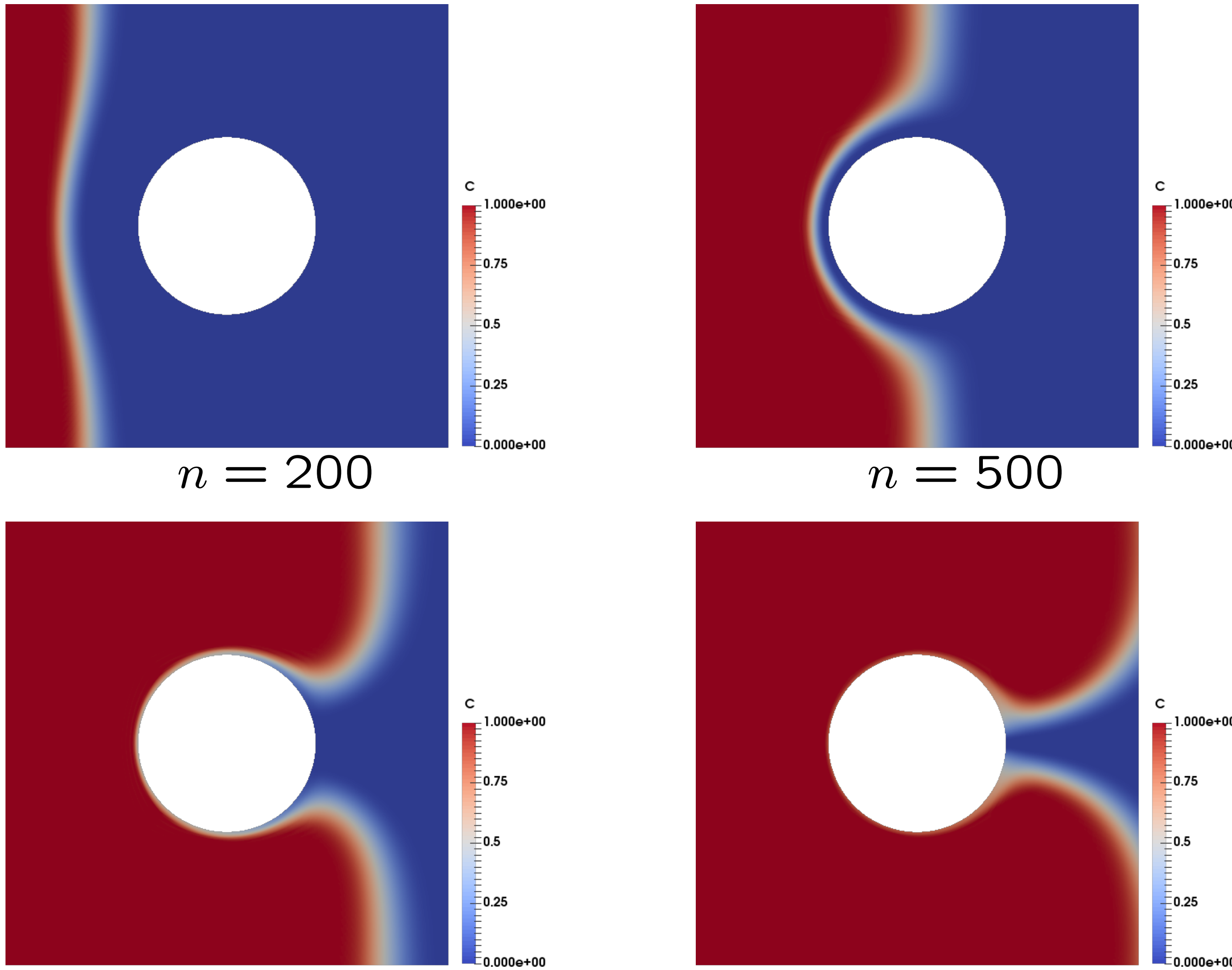

$n = 200$ $n = 500$

$n = 800$ $n = 1000$

Similar to Sun and Liu 2009 (but we use many fewer DoFs) and Lee, Lee & Wheeler 2016 (but we follow a round hole)

III. Discontinuous Finite Volume WENO Approximations

The solution may have a shock or steep front
(conforming finite elements are less effective in this case)

Advantages of Finite Volume WENO Methods

Discontinuous Galerkin places many DoFs inside each mesh element E to understand solution behavior on ∂E.

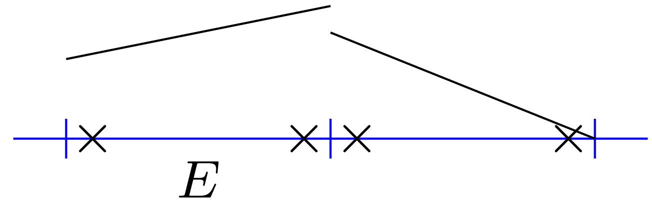

Finite Volume places one DoF inside each mesh element, and looks outside E to find solution behavior on ∂E.

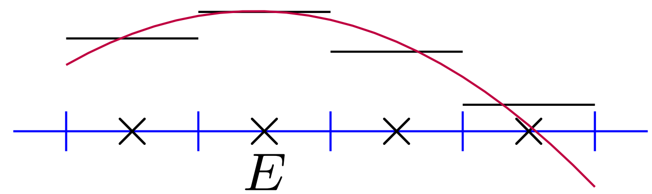

1. Uses one degree of freedom per element:
   - in any space dimension,
   - for any degree of approximation.
2. Maximizes the mesh resolution of the heterogeneity.
   For porous media, permeability and porosity are constant on an element but vary greatly between elements.
3. The mesh needs no special properties.
4. WENO is *essentially* non-oscillatory. (Use flux corrected transport?)

We address certain **practical issues** that reduce the popularity of finite volume methods for solving advection-diffusion problems.

The Gibbs Phenomenon

Approximation of a jump discontinuity by Fourier Series leads to oscillation, with overshoot and undershoot of about a 9%.

True also for other approximations: polynomials, splines, wavelets, etc.

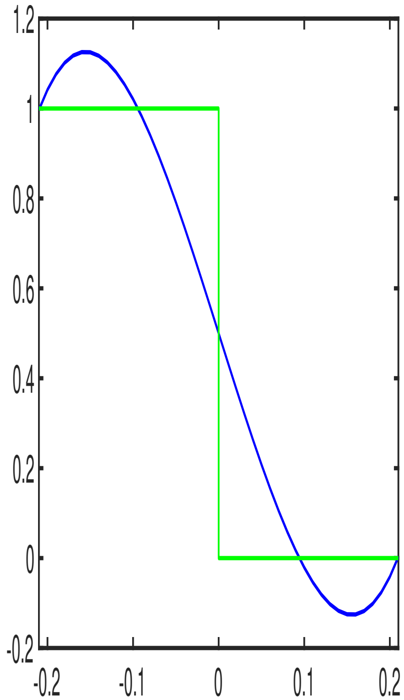

Degree 5 polynomial

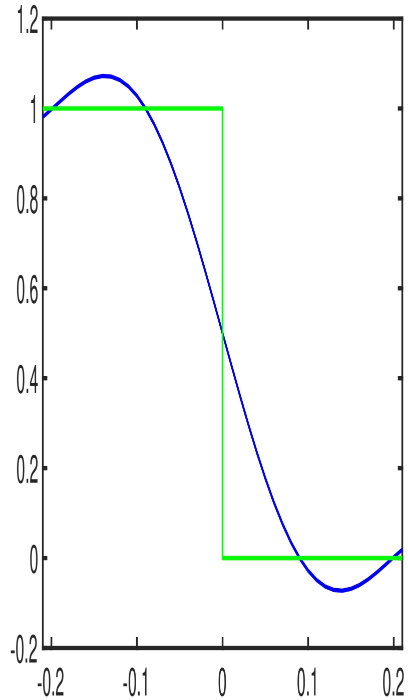

Degree 11 polynomial

Our reconstruction should not cross a shock

The Equation in Finite Volume Form

$$\boxed{u_t + \nabla \cdot [f(u) - D(u)\nabla u] = q(u)}$$

Finite volumes. Average over mesh elements $E \subset \mathbb{R}^2$

$$\bar{u}_E(t) = \frac{1}{|E|}\int_E u(x,t)\,d\mathbf{x} \quad (|E| \text{ is the area of } E)$$

The averaged equation. Mass conservation over E is

$$\bar{u}_{E,t} + \frac{1}{|E|}\int_E \nabla \cdot [f(u) - D(u)\nabla u]\,d\mathbf{x} = \frac{1}{|E|}\int_E q(u)\,d\mathbf{x}$$

Apply the Divergence Theorem to find

$$\boxed{\bar{u}_{E,t} + \frac{1}{|E|}\int_{\partial E} \big(f(u) - D\nabla u\big) \cdot \nu_E\,ds(\mathbf{x}) = \frac{1}{|E|}\int_E q(u)\,d\mathbf{x}}$$

A numerical flux function for the advective term is needed

- to stabilize the computations (by adding numerical diffusion)
- to account for potential discontinuities in the solution

Lax-Friedrichs numerical flux

$$\widehat{f}_E(u^-,u^+) = \frac{1}{2}\Big[(f(u^-)+f(u^+))\cdot\nu_E - \alpha_{\mathsf{LF}}(u^+-u^-)\Big]$$

- u^- and u^+ are left and right limits of the solution at the interface ∂E
- $\alpha_{\mathsf{LF}} = \max\limits_u \left|\partial f/\partial u\right|$ (maximum wave speed)

$$u^- < u^+ \qquad u^- > u^+$$

- if u is continuous, we have consistency with the original flux

$$\widehat{f}_E(u,u) = f(u)\cdot\nu_E$$

The finite volume equation. Thus

$$\bar{u}_{E,t} + \frac{1}{|E|}\int_{\partial E}\left[\hat{f}_E(u^-,u^+) - D(u)\nabla u\cdot\nu_E\right]ds(\mathbf{x}) = \frac{1}{|E|}\int_E q(u)\,d\mathbf{x}$$

Approximate time evolution.

- Use a Runge-Kutta time integrator

Approximate spatial variation.

- Approximate u from its element averages $\bar{u}_E^n$.
  Use stencil polynomials defined on stencils of mesh cells.
- Combine the stencil polynomials.
  Use a (new) weighted essentially non-oscillatory (WENO) reconstruction to avoid shocks and steep fronts.
- Approximate $u^{\pm}(\mathbf{x})$ and $D(u)\nabla u\cdot\nu_E(\mathbf{x})$ using the reconstruction.

1. Stencil Polynomial Approximations

Can we guarantee good accuracy?

Construction of Stencil Polynomials

(Harten & Chakravarthy 1991, Abgrall 1994)

1. Select a stencil $S = \{E_j,\ \text{some } j\}$ of mesh elements

2. Find $P(\mathbf{x}) = \sum_{\alpha<r} c_\alpha \left(\frac{\mathbf{x}-\mathbf{x}_S}{h_S}\right)^\alpha$, polynomial of degree $r-1$.

   - Match averages

$$\frac{1}{|E_j|}\int_{E_j} P(\mathbf{x})\,d\mathbf{x} = \bar{u}_{E_j} \qquad \Longleftrightarrow \qquad A\mathbf{c} = \mathbf{u}$$

   - Requires least-squares fitting (usually)

$$N = \text{number of polynomial coefficients}$$
$$\neq M = \text{number of stencil elements}$$

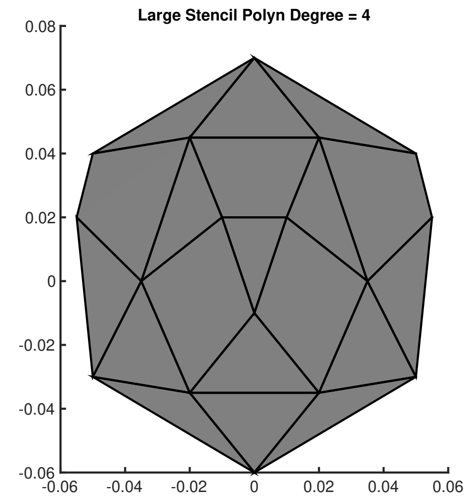

3. Find the SVD decomposition and the singular values

$$A = U\Sigma V^T, \quad s_1 \geq s_2 \geq \cdots \geq s_M$$

4. $\mathbf{c} = (A^TA)^{-1}A^T\mathbf{u} = V\Sigma^{-1}U^T\mathbf{u}$
   (actually *constrained* least-squares: match averages of target cell)

We have defined a linear projection operator $\pi : u \mapsto \pi u = P$

We expect accuracy $|u(\mathbf{x}) - P(\mathbf{x})| \le Ch^r$

Bramble-Hilbert Lemma (Bramble & Hilbert 1970, Dupont & Scott 1980)

P will accurately approximate $u(\mathbf{x})$ and its derivatives provided

- u is smooth on the stencil (if there is no shock!)
- π preserves polynomials (it clearly does)
- π is a bounded operator (it will be as long as the matrix $A^T A$ is well conditioned and the mesh is quasiuniform)

Continuing the algorithm (A., Huang, Tian 2024)

5. Reject the polynomial if the condition number $(s_1/s_M)^2 \gg 1$. Decrease r and try again. Terminate at $r \ge 1$ ($P =$ constant).

Results in the best polynomial approximation for the given stencil

Efficiency. Reuse the stencils each time step.

- Determine r and precompute $A = U\Sigma V^T$ once before the time loop.
- Each time step set the coefficients $\mathbf{c} = (A^T A)^{-1} A^T \mathbf{u} = V\Sigma^{-1} U^T \mathbf{u}$.

Examples of Bad Stencils

Singular stencil. 6 elements, $\dim \mathbb{P}_2 = 6$

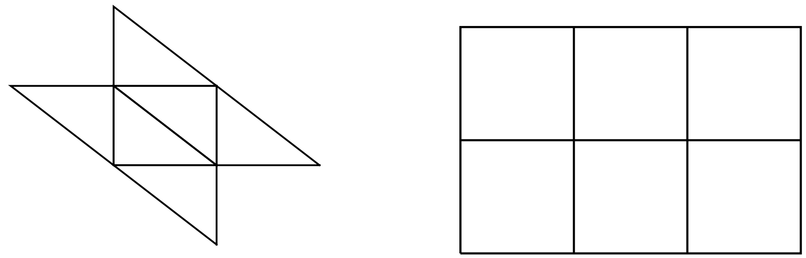

A good stencil.

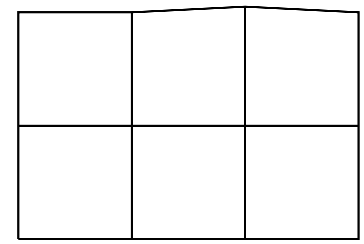

A badly conditioned stencil. 15 elements

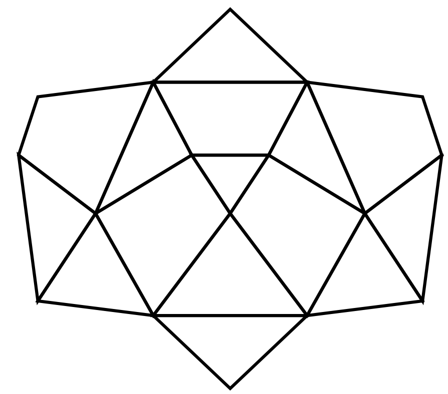

- $\dim \mathbb{P}_4 = 15$, s_1=3.8809, s_{15}= 7.6840e-11
  Condition number = 5.05e+10
- $\dim \mathbb{P}_3 = 10$, s_1=3.8808, s_{10}=9.4274e-03
  Condition number = 4.12e+2

$2(1+\cos(2\pi x))\exp(xy-y)$ refinement level	$\mathbb{P}_4$ polynomial L1-error	Rate	$\mathbb{P}_3$ polynomial L1-error	Rate
0	4.124e+07	——	5.697e-06	——
1	1.291e+06	5.00	3.550e-07	4.00
2	4.036e+04	5.00	2.218e-08	4.00
3	1.261e+03	5.00	1.386e-09	4.00
4	3.947e+01	5.00	8.658e-11	4.00

2. New ML-WENO Reconstruction

WENO Reconstruction

Use many stencils with the same target element E

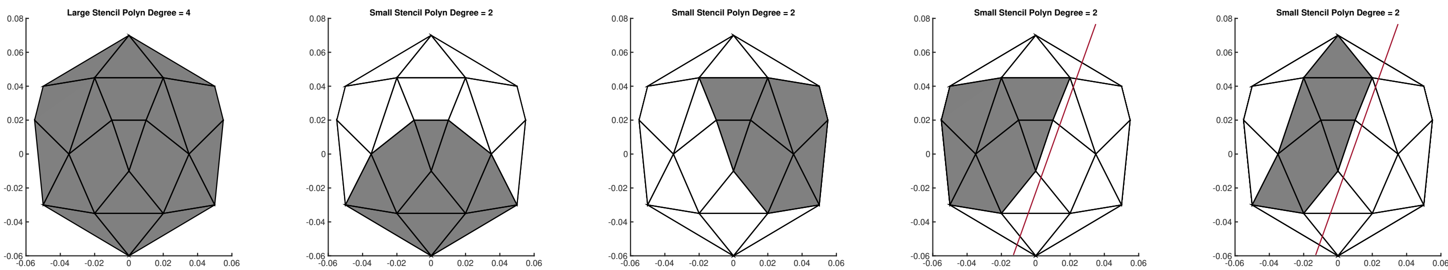

- For $P_\ell \in \mathbb{P}_{r_\ell - 1}$

$$R(\mathbf{x}) \sim \sum_{\ell} \omega_\ell P_\ell(\mathbf{x}) \qquad \text{(linearly weighted average)}$$

- Measure the smoothness σ_ℓ of P_ℓ
- Use σ_ℓ to bias away from stencil polynomials that cross shocks

$$R(\mathbf{x}) = \sum_{\ell} \tilde{\omega}_\ell P_\ell(\mathbf{x}) \qquad \text{(nonlinearly weighted average)}$$

Challenges. Current techniques require:

- Polynomials of only two degrees, or stencils arranged hierarchically
- non-constant polynomials

We need to be able to use any set of stencils and polynomials

Reconstruction of u:

$$R(\mathbf{x}) = \sum_{\ell} \tilde{\omega}_\ell P_\ell(\mathbf{x}) \qquad \text{(weighted average)}$$

Smoothness Indicator. (Jiang & Shu 1996, Friedrichs 1998)

For $P(x) \in \mathbb{P}_{r-1}$ $(h_0 = \mathrm{diam}(E_0))$

$$\sigma_P = \sum_{1 \le |\alpha| \le r-1} \frac{h_0^{2|\alpha|}}{|E_0|} \int_{E_0} \big(\mathcal{D}^\alpha P(\mathbf{x})\big)^2 d\mathbf{x}$$

A scaled L^2-Sobolev seminorm squared

Lemma. As $h \to 0^+$, there is $D \ge 0$ such that

$$\sigma_P = \begin{cases} D h_0^2 + \mathcal{O}(h^3) & \text{if } u \text{ is smooth on the stencil} \\ \mathcal{O}(1) & \text{if } u \text{ has a jump discontinuity} \end{cases}$$

New ML-WENO (Multi-Level Weighting)

For linear weights $\omega_\ell > 0$, use nonlinear weights

$$\tilde{\omega}_\ell = \frac{\widehat{\omega}_\ell}{\sum_{k\geq 0} \widehat{\omega}_k} \quad \text{where} \quad \widehat{\omega}_\ell = \frac{\omega_\ell}{(\sigma_{P_\ell} + \epsilon_0 h^2)^{r_\ell}} \quad \text{in} \quad R(\mathbf{x}) = \sum_\ell \tilde{\omega}_\ell P_\ell(\mathbf{x})$$

Theorem. For all $\mathbf{x} \in E$ (the target element)

$$|u(\mathbf{x}) - R(\mathbf{x})| \leq C h^{r_{\max}}$$

where $r_{\max} = \max_\ell \{r_\ell : u \text{ is smooth on the } \ell\text{th stencil}\}$

$$\boxed{r_{\max} = \text{highest order of accuracy of stencils without a shock}}$$

Advantages.

- Handles smooth and discontinuous solutions
- Uses any stencils (chosen to capture shocks)
- Uses any order stencil polynomials (including constants)
- Gives the best approximation while avoiding shocks

- Smoothness indicator $$\sigma_P = \begin{cases} Dh_0^2 + \mathcal{O}(h^3) & \text{if } u \text{ smooth} \\ \Theta(1) & \text{if } u \text{ jumps} \end{cases}$$
- Weight scaling $$\hat{\omega}_\ell = \frac{\omega_\ell}{(\sigma_{P_\ell} + \epsilon_0 h^2)^{r_\ell}} = \begin{cases} \mathcal{O}(h^{-2r_\ell}) & \text{if } u \text{ smooth} \\ \Theta(1) & \text{if } u \text{ jumps} \end{cases}$$
- Nonlinear weights $$\tilde{\omega}_\ell = \frac{\hat{\omega}_\ell}{\sum_{k\geq 0} \hat{\omega}_k} = \begin{cases} \Theta(h^{2(r_{\max}-r_\ell)}) & \text{if } u \text{ smooth} \\ \Theta(h^{2r_{\max}}) & \text{if } u \text{ jumps} \end{cases}$$
- Error estimation

$$\begin{aligned} |u(\mathbf{x}) - R(\mathbf{x})| &= \left| \sum_\ell \tilde{\omega}_\ell \big(u(\mathbf{x}) - P_\ell(\mathbf{x}) \big) \right| \\ &\leq \sum_\ell \tilde{\omega}_\ell \big| u(\mathbf{x}) - P_\ell(\mathbf{x}) \big| \\ &= \underbrace{\sum_\ell \Theta(h^{2(r_{\max}-r_\ell)}) h^{r_\ell}}_{u \text{ smooth on stencil } \ell} + \underbrace{\sum_\ell \Theta(h^{2r_{\max}}) \mathcal{O}(1)}_{u \text{ discontinuous on stencil } \ell} = \Theta(h^{r_{\max}}) \end{aligned}$$

Stencil polynomial of degree 4 and 0 (19 elements and 1 target element)

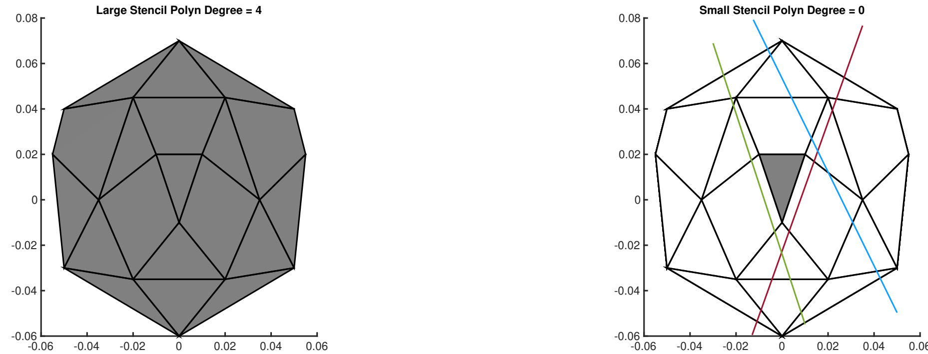

Stencil polynomials of degree 2 (9, 7, 7, 6 elements)

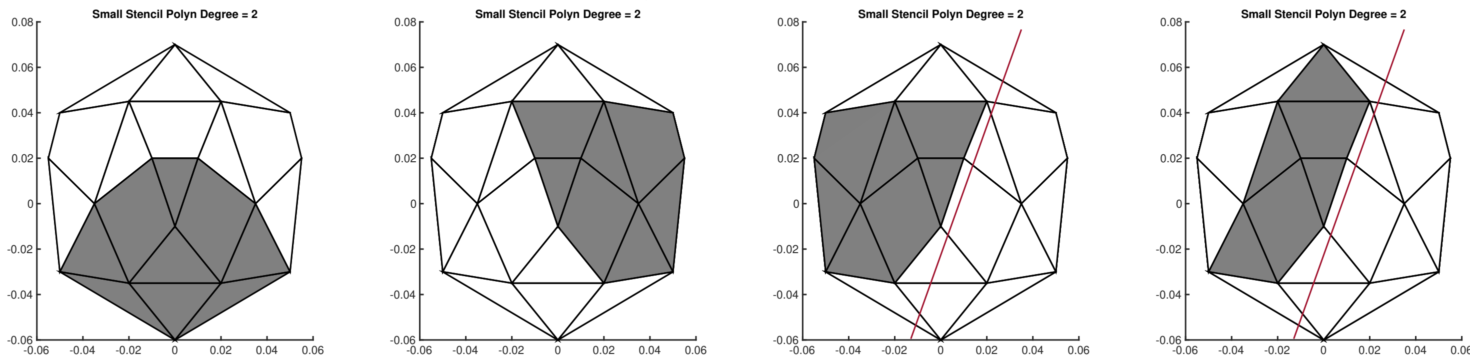

Stencil polynomials of degree 1 (3, 3, 3 elements)

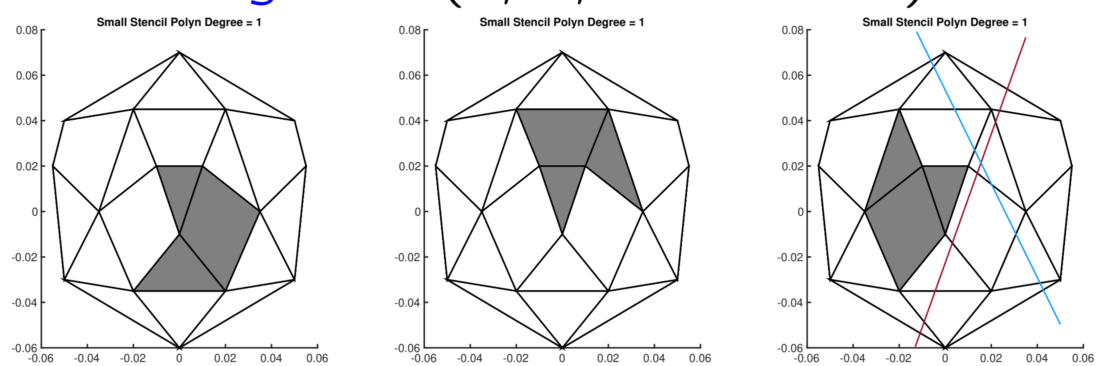

Four tests with $u(x,y) = 2(1+\cos(2\pi x))\exp(xy-y) + \text{jump}$

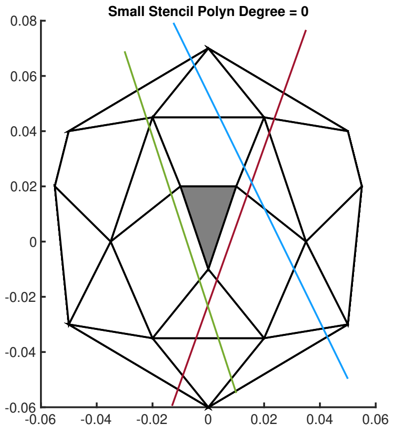

- $\mathcal{O}(h^1)$, green & blue jump lines cut all but constant
- $\mathcal{O}(h^2)$, blue jump cuts all degree 2, not all degree 1
- $\mathcal{O}(h^3)$, red jump does not cut one stencil of degree 2
- $\mathcal{O}(h^5)$, no jump

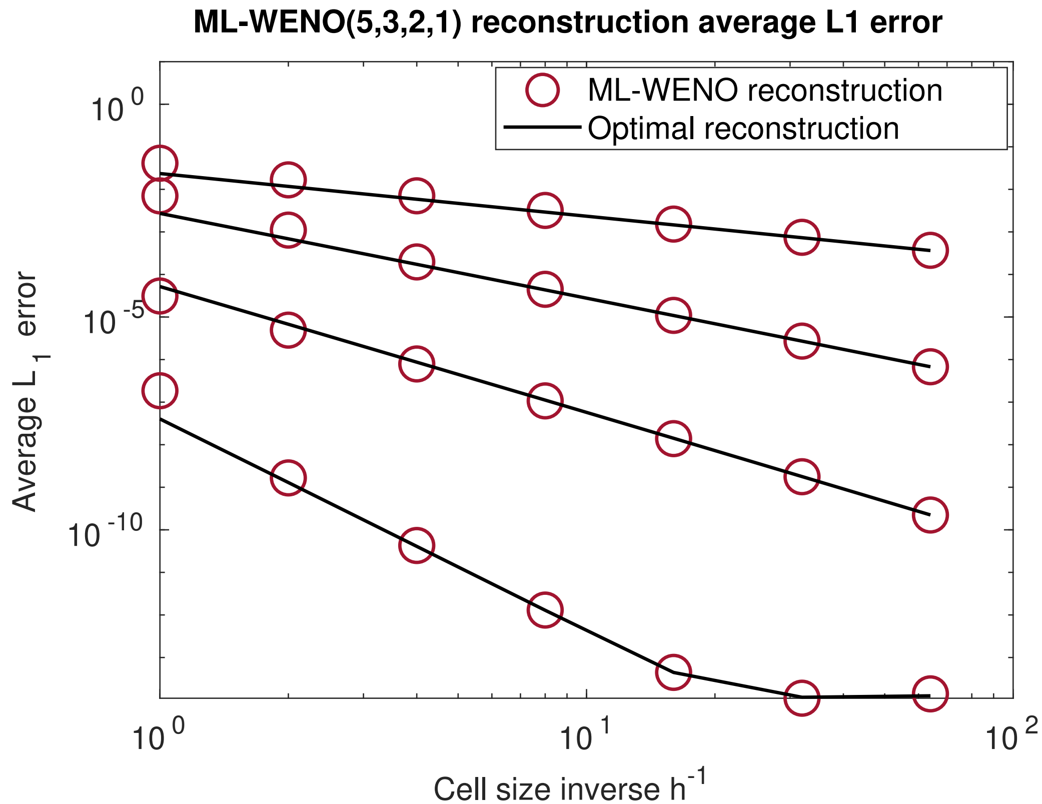

For edge e of the mesh, we need to compute (by quadrature)

$$\int_e D(u)\nabla u \cdot \nu \, d\mathbf{x}$$

Kirchhoff Transformation. $D(u)$ may be degenerate, so if possible, define

$$b(u) = \int_0^u D(v)\,dv \qquad \Longrightarrow \qquad \nabla b(u) = D(u)\nabla u$$

Procedure. At a quadrature point of $e = E_1 \cap E_2$

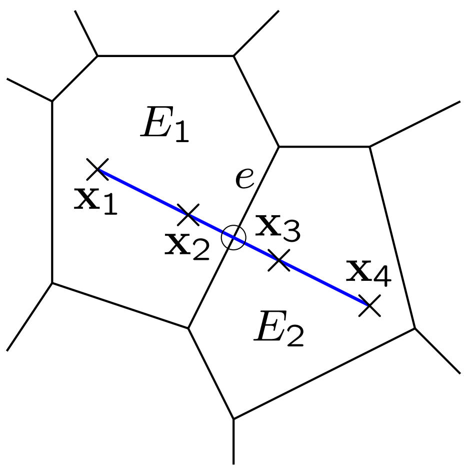

Line normal to e

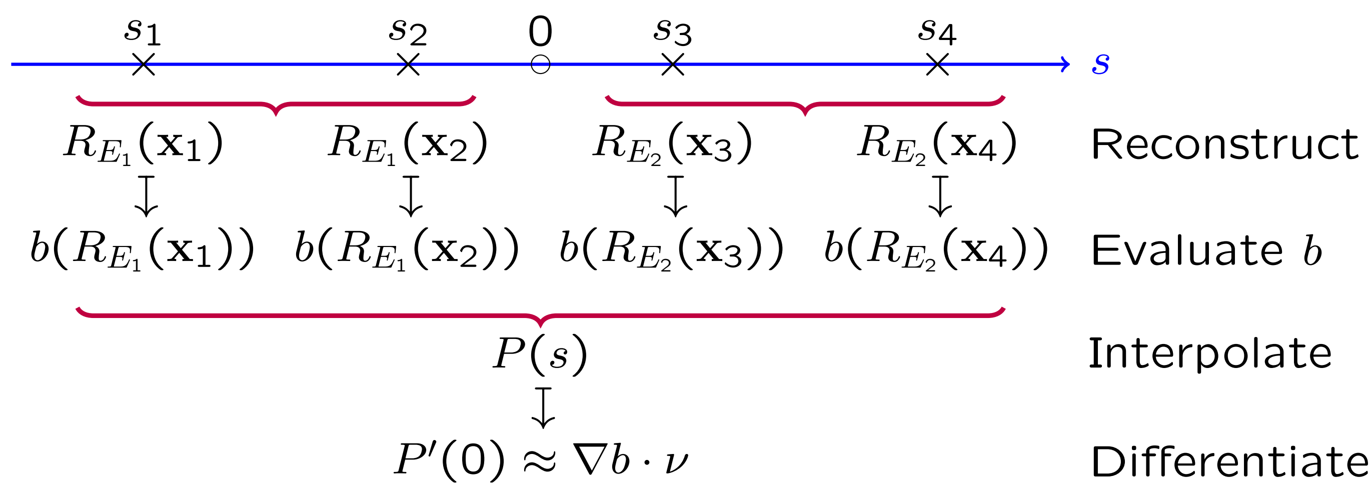

Remarks.

- If no Kirchhoff: $b(u) = u$ and $D(u)\nabla u \cdot \nu \approx D(R(\mathbf{x}))P'(0)$
- The computations are in 1D for any spatial dimension.

3. Some Numerical Results

Random 2D Mesh

- About 50×50
- Mostly quadrilaterals, some triangles
- Large stencil polynomials of degree 5 or 4 (order drops automatically)
- Small stencil polynomials of degree 2

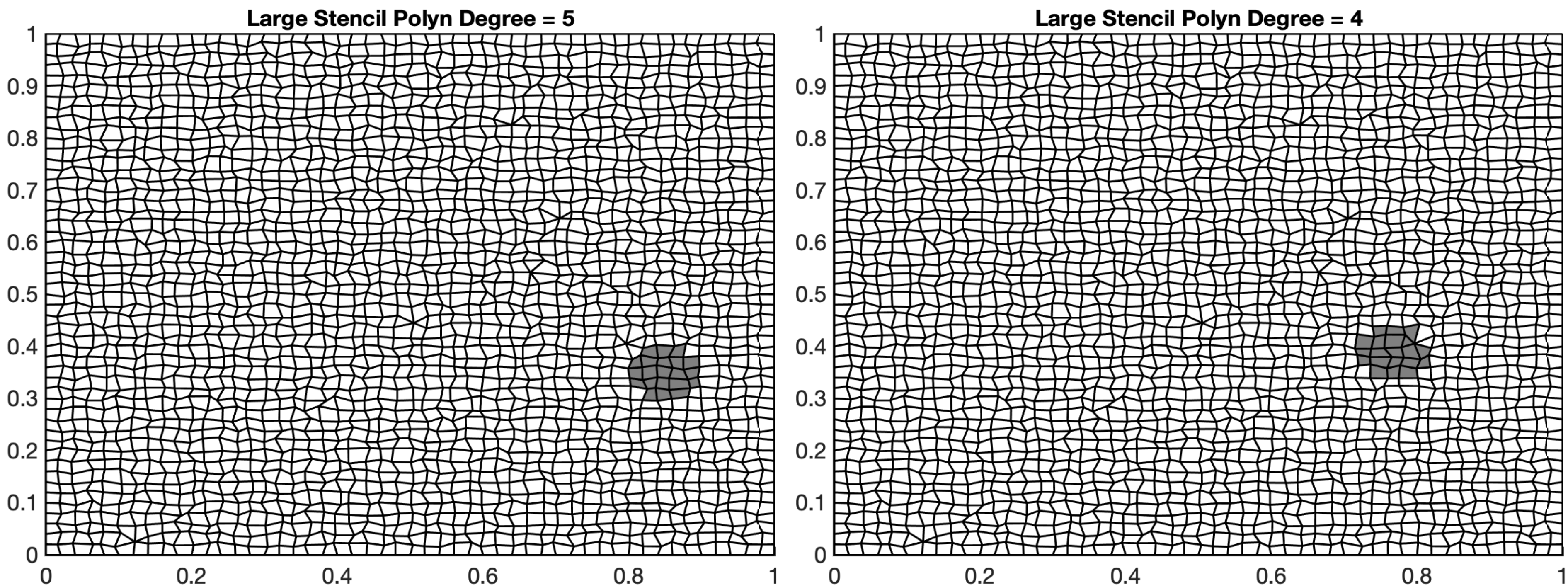

Remark. Minimal DoFs of FV allows a fine mesh.

FEM and DG would use a mesh with elements the size of the stencil, which would be about 10×10 (for the same number of DoFs).

Burgers Equation

$$\boxed{u_t + (u^2/2)_x + (u^2/2)_y = 0}$$

Shock formation. $u(x, y, 0) = (\sin(\pi x)\sin(\pi y))^2$, $(x, y) \in [0, 1]^2$
Periodic BCs, $\Delta t = 0.002$ (CFL ≈ 0.1)

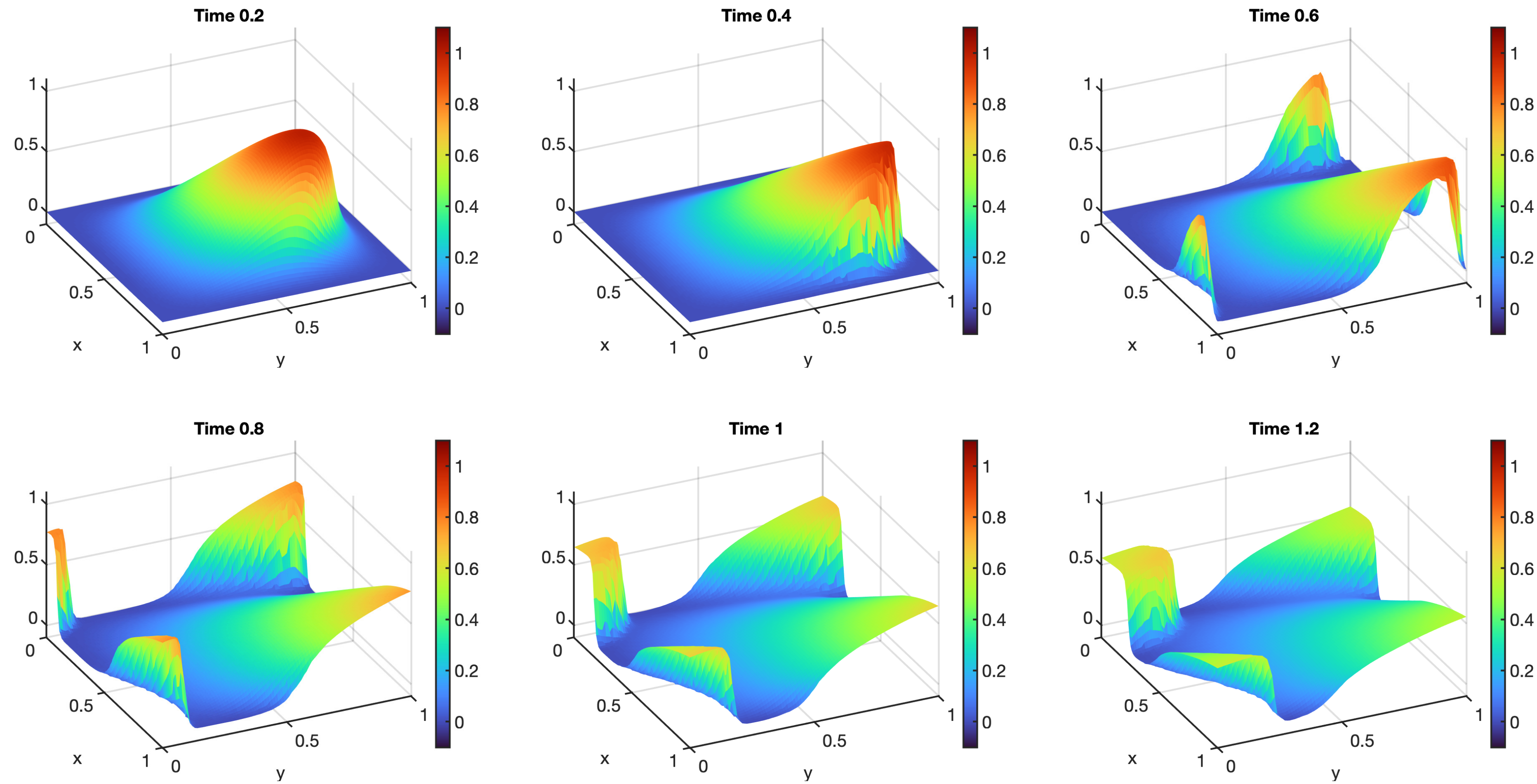

Graphs of the reconstructed solution

Linear Flux, Rotating Flow

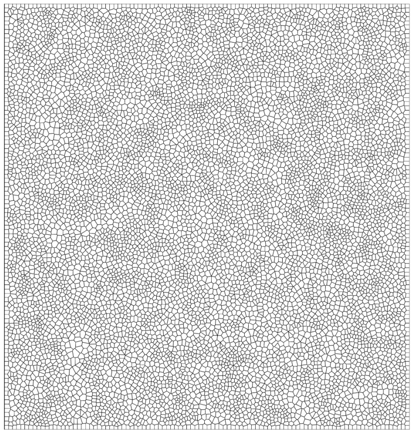

$$f(u) = (0.5 - y, x - 0.5)u$$

A polygonal mesh of 10,000 cells
One revolution (10,000 timesteps)
WENO(5,4,3,2) reconstructions

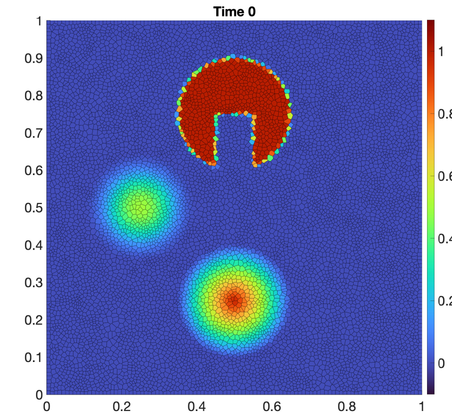

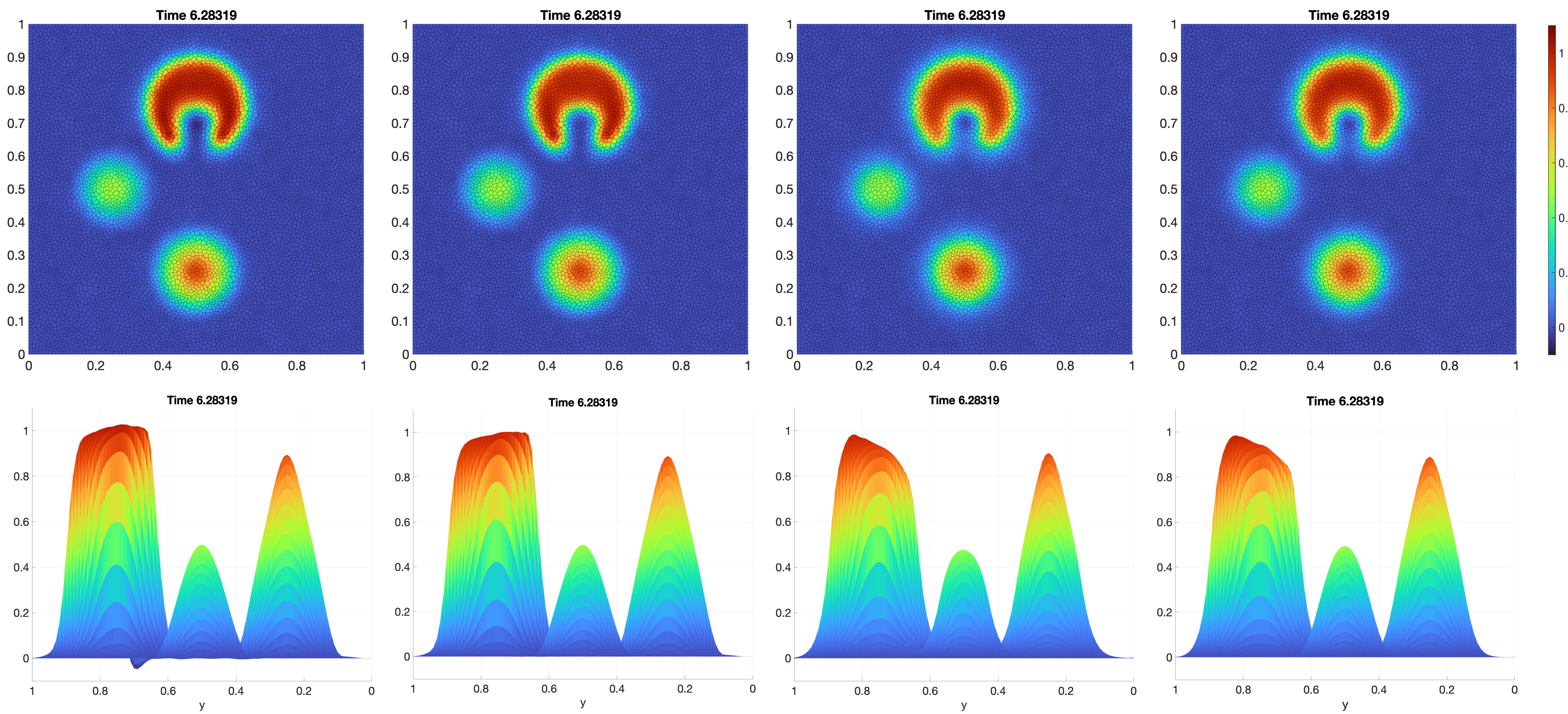

ML-WENO
L^1 err 1.83e-02

ML-WENO (FC)
L^1 err 1.89e-02

WENO-AO
L^1 err 2.69e-02

WENOZ-AO
L^1 err 2.38e-02

Porous Medium Equation in 2D

$$\boxed{u_t = \Delta u^m} \quad \text{(degenerate diffusion)}$$

Initial condition is two round bumps.

$$u(x,y,0) = \begin{cases} \exp\big(-1/[6-(x-2)^2-(y+2)^2]\big), & \text{if } (x-2)^2+(y+2)^2 < 6 \\ \exp\big(-1/[6-(x+2)^2-(y-2)^2]\big), & \text{if } (x+2)^2+(y-2)^2 < 6 \\ 0, & \text{otherwise} \end{cases}$$

PME at $t = 1$ with $m = 2$ using $M = 40$ elements and $\Delta t = h/2$

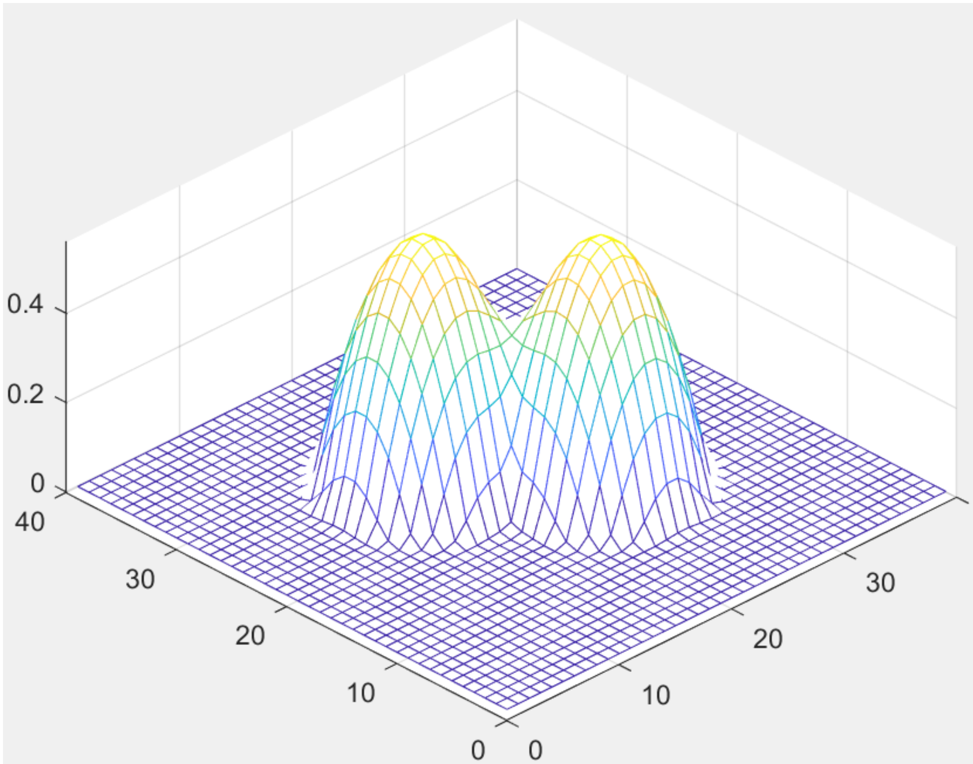

Free outflow Boundary Condition

Wave traveling diagonally under linear transport

- Cut Stencils: Stencils near the boundary are cut off.
- Extra Stencils: Add stencils near the outflow boundary.

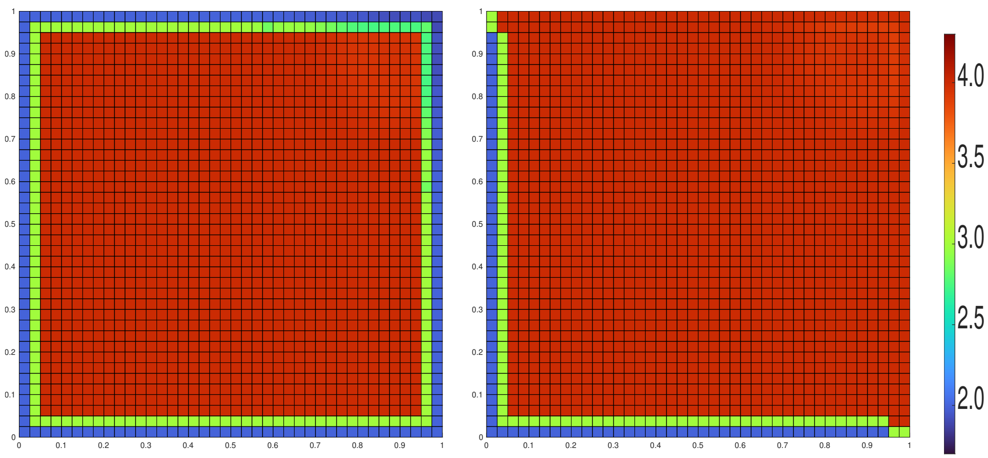

Cut stencils   Extra Stencils

Effective polynomial degree

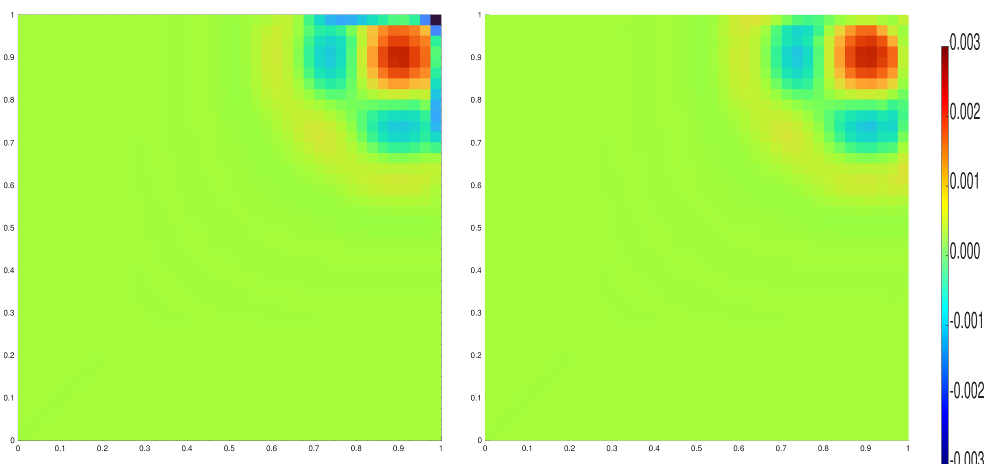

Cut Stencils   Extra Stencils

Error distribution

ML-WENO(5,4,3,2)

	Cut stencils		Extra Stencils	
mesh size	$L^\infty(L^1)$-error	rate	$L^\infty(L^1)$-error	rate
20×20	4.41e-03	—	4.26e-03	—
40×40	1.19e-04	5.21	1.05e-04	5.34
80×80	5.05e-06	4.67	3.82e-06	4.78
160×160	2.17e-07	4.54	1.25e-07	4.93
250×250	2.99e-08	4.44	1.36e-08	4.97

Incoming shock wave for $u_t + u^3 u_x = 0$

ML-WENO(5,4,3,2).

No special treatment of the boundary.

- Linear reconstruction near the inflow boundary causes overshoot.
- Unstable after time 0.075

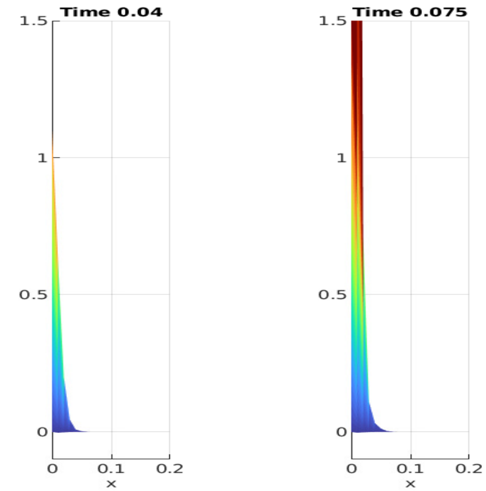

ML-WENO(5,4,3,2,1). Add constant polynomials near inflow boundary.

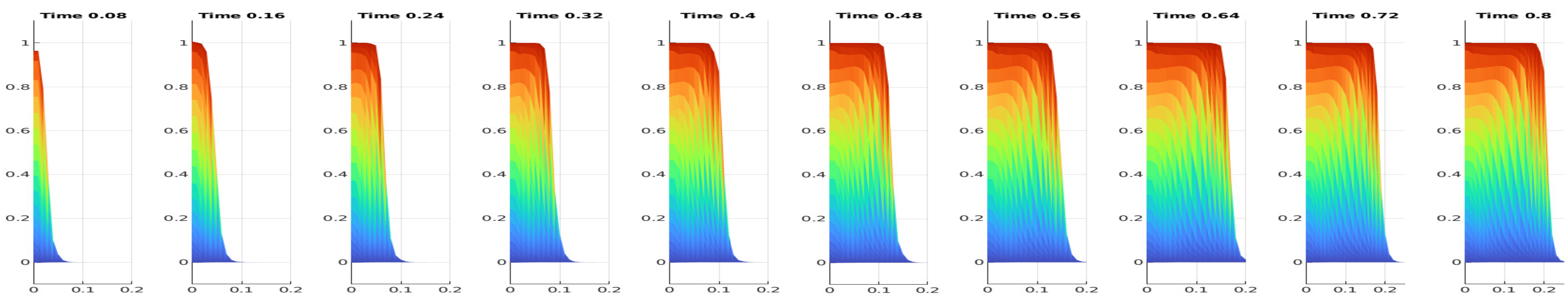

- Constant reconstruction near inflow gives almost no overshoot.
- Shock wave is clean, sharp, and stable.

4. Preliminary Application to Two-Phase Flow (Richards Equation)

Air-water system assuming infinitely mobile air connected to the surface

$$\phi s_t + \nabla \cdot \mathbf{v}_\mathrm{w} = q(s)$$
$$\mathbf{v}_\mathrm{w} = -\lambda_\mathrm{w}(s)\, K\, (\nabla p_\mathrm{w} - \rho_\mathrm{w}\, \mathbf{g})$$
$$p_\mathrm{c}(s) = -p_\mathrm{w} \le 0 \qquad (p_\mathrm{n} = 0 \text{ by assumption})$$

Unknown solution

- s water saturation
- p_w water pressure
- $\mathbf{v}_w$ water velocity

Data

- ϕ porosity
- K permeability
- λ_w relative mobility
- ρ_w water density
- $\mathbf{g}$ gravity vector
- p_c capillary pressure
- q external wells

Kirchhoff Transformation.

$$D(s) = -\int_0^s \lambda_\mathrm{w}(S) p_\mathrm{c}'(S)\, dS \qquad \Longrightarrow \qquad \nabla D(s) = -\lambda_\mathrm{w}(s) \nabla p_\mathrm{c}(s) = \lambda_\mathrm{w}(s) \nabla p_w$$

Eliminate: $p_\mathrm{w} = -p_\mathrm{c}(s)$ and $\mathbf{v}_\mathrm{w} = -K \nabla D(s) + \rho_\mathrm{w}\, \lambda_\mathrm{w}(s)\, K\, \mathbf{g}$

$$\boxed{\phi s_t \underbrace{- \nabla \cdot \Big(K \nabla D(s)\Big)}_{\text{diffusion}} + \underbrace{\nabla \cdot \Big(\rho_\mathrm{w}\, \lambda_\mathrm{w}(s)\, K\, \mathbf{g}\Big)}_{\text{advection}} = q(s)}$$

Algorithm. Advance time by a Runge-Kutta method.

- $\bar{s}^{n,0} = \bar{s}^n$
- For each Runge-Kutta stage

$$\bar{s}^{n,\ell} \xmapsto{\text{ML-WENO}} R^{n,\ell} \xmapsto{\text{Point evaluation}} (s^{n,\ell}, p_{\mathrm{W}}^{n,\ell}, \mathbf{v}_{\mathrm{W}}^{n,\ell}) \xmapsto{\text{Transport}} \bar{s}^{n,\ell+1}$$

- $\bar{s}^{n+1} = \bar{s}^{n,\ell_{\max}}$

Remarks.

- We use a single rock type and constant porosity, so s is smooth except for steep fronts.
- The scheme is not well-balanced with respect to gravitational equilibrium on general meshes.
- We should solve for the smoother variable p_{W}. But then

$$\bar{p}_{\mathrm{W}}^{n,\ell} \xmapsto{\text{ML-WENO}} R^{n,\ell} \xmapsto{\text{Point evaluation}} (s^{n,\ell}, p_{\mathrm{W}}^{n,\ell}, \mathbf{v}_{\mathrm{W}}^{n,\ell})$$
$$\xmapsto{\text{Transport}} \bar{s}^{n,\ell+1} \xmapsto{\text{Transform}} \bar{p}_{\mathrm{W}}^{n,\ell+1}$$

- Only explicit Runge-Kutta at this time.

Preliminary Numerical Result

- $100\,\mathrm{m} \times 10\,\mathrm{m}$
- 100×50 quadrilateral mesh
- 6000 steps using explicit Euler (similar results for SSP3)
- $\Delta t = 0.001$ days
- van Genuchten capillary and water mobility curves

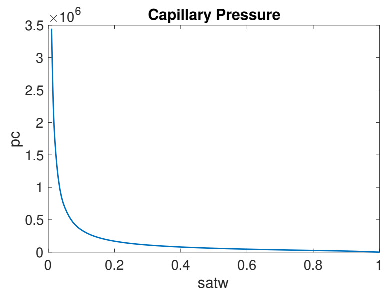

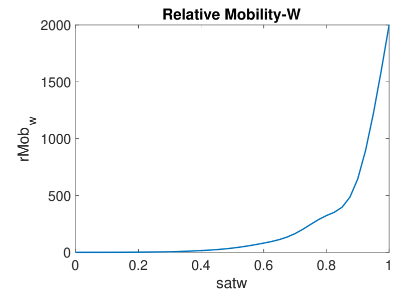

- Heterogeneous permeability (about 0.1 to 1 Darcy)

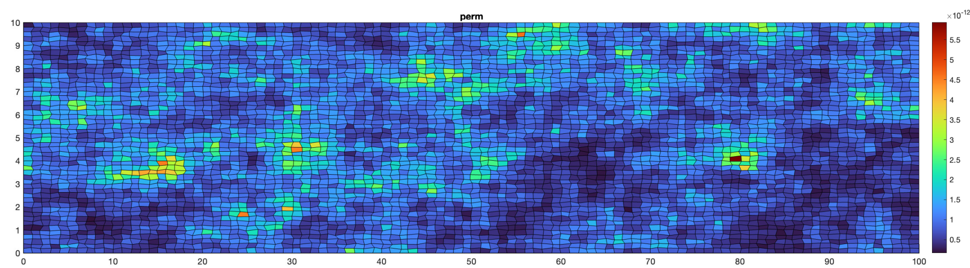

- Continuous infiltration of water at the surface

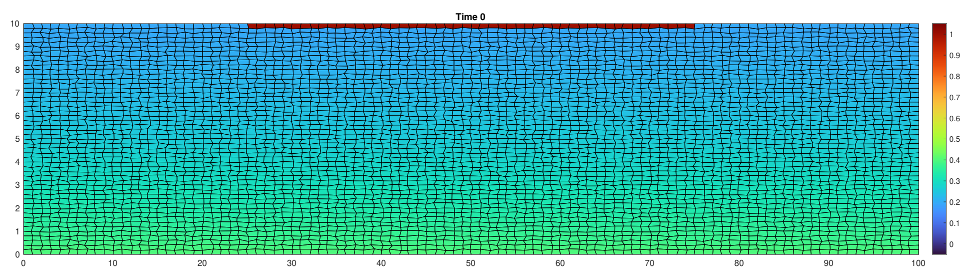

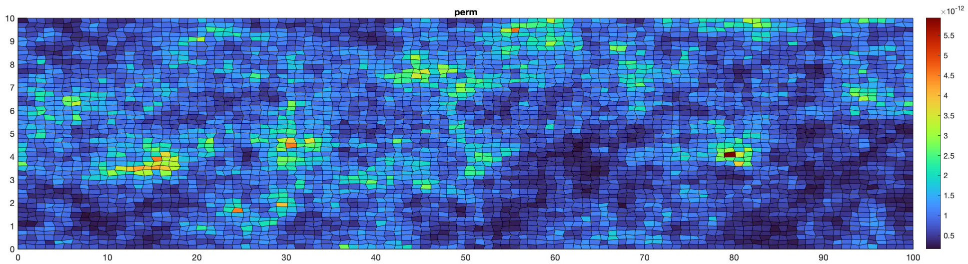

Permeability

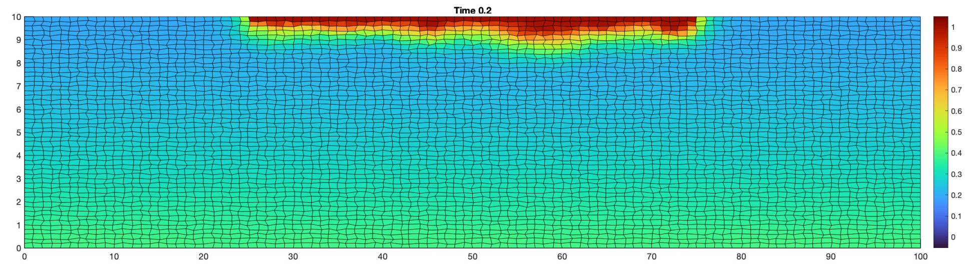

ML-WENO(1)

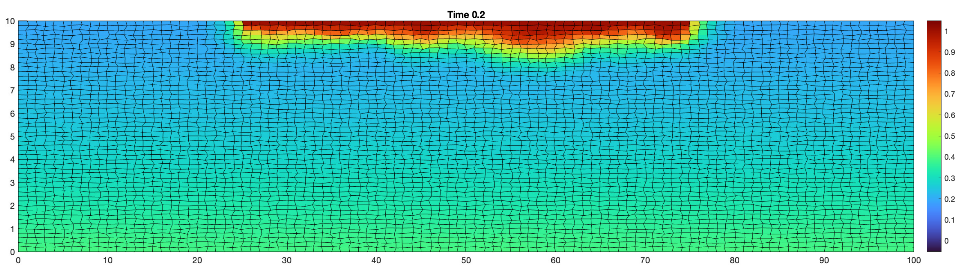

ML-WENO(2,1)

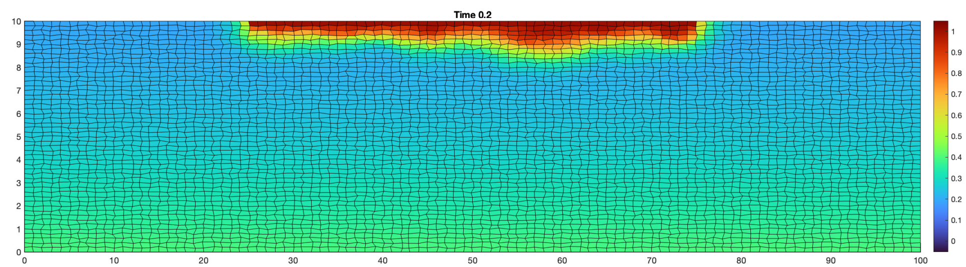

ML-WENO(3,1)

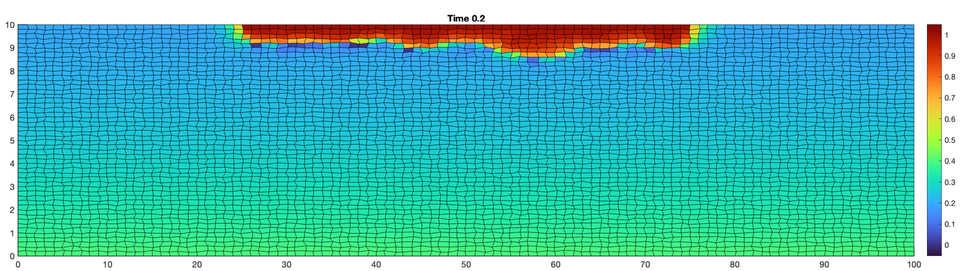

ML-WENO(3,2)

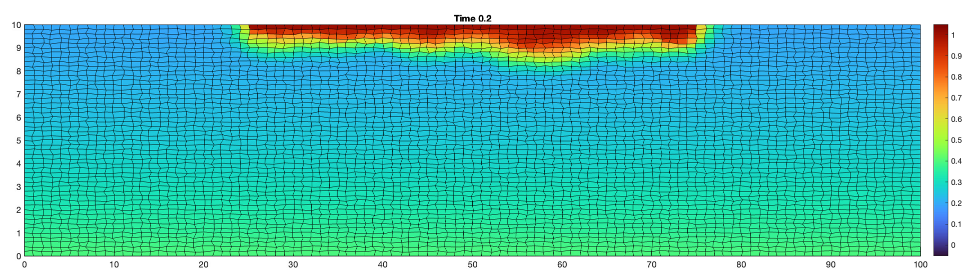

ML-WENO(3,2,1)

Day 0.2

Infiltration of Water at the Surface—1 day

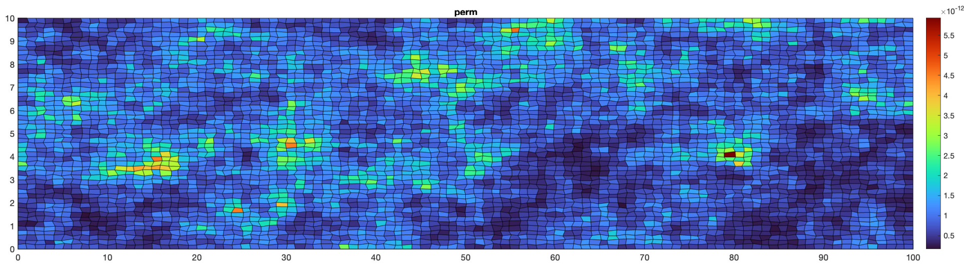

Permeability

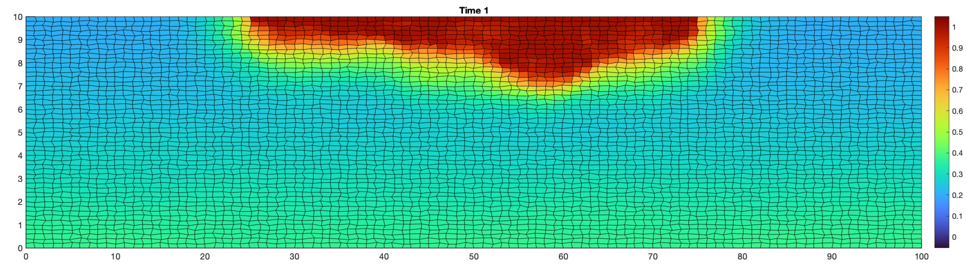

ML-WENO(1)

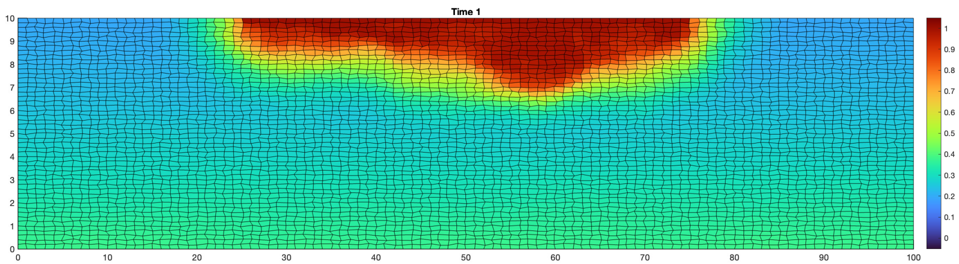

ML-WENO(2,1)

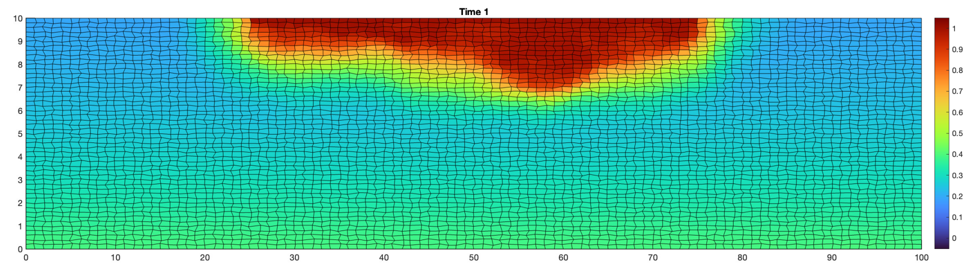

ML-WENO(3,1)

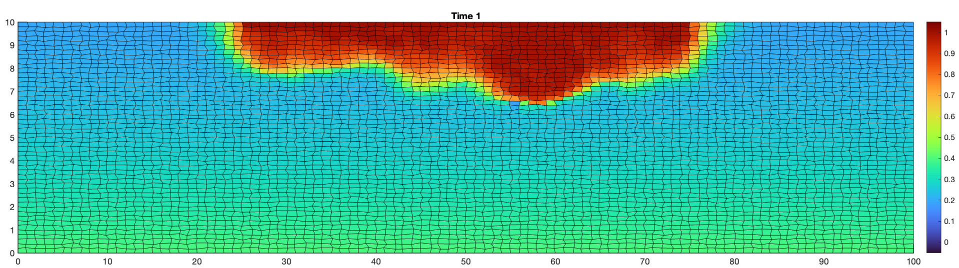

ML-WENO(3,2)

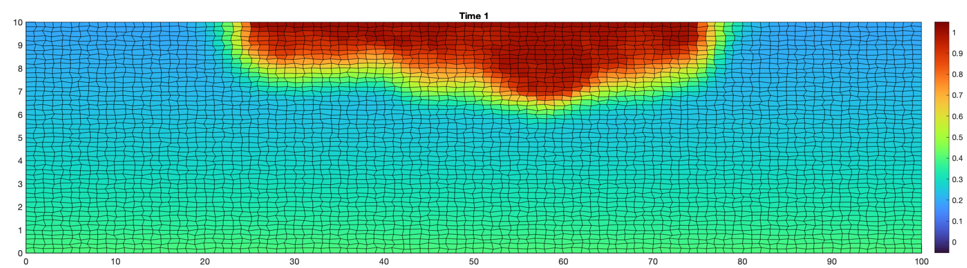

ML-WENO(3,2,1)

Day 1

Infiltration of Water at the Surface—2 days

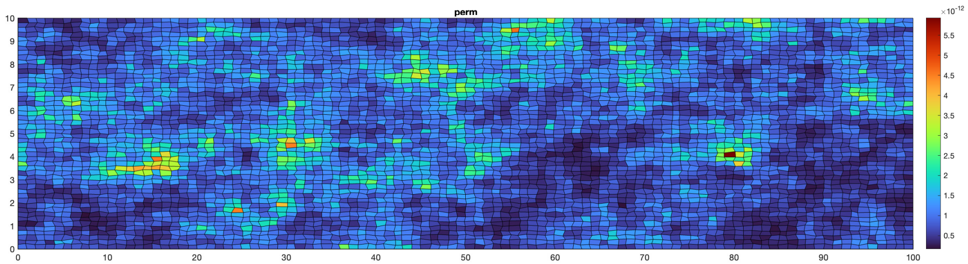

Permeability

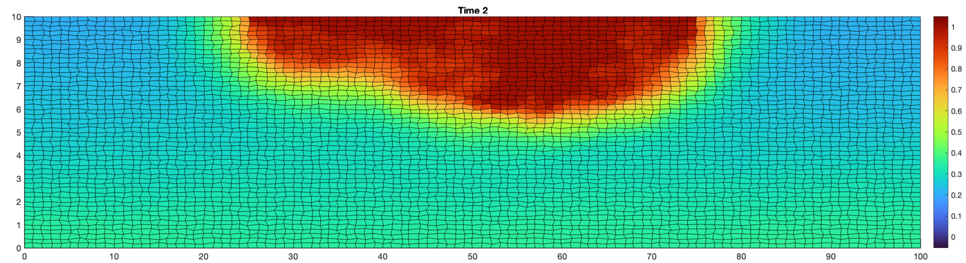

ML-WENO(1)

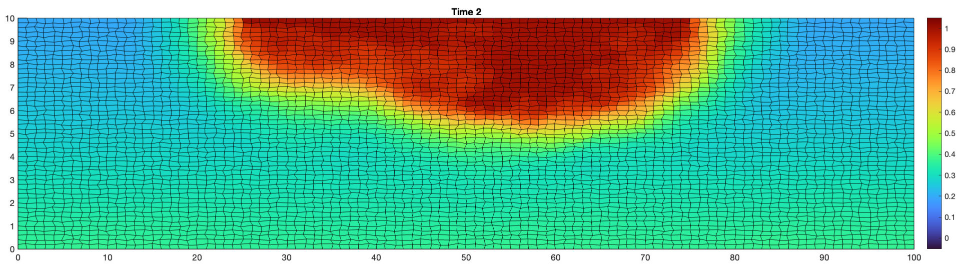

ML-WENO(2,1)

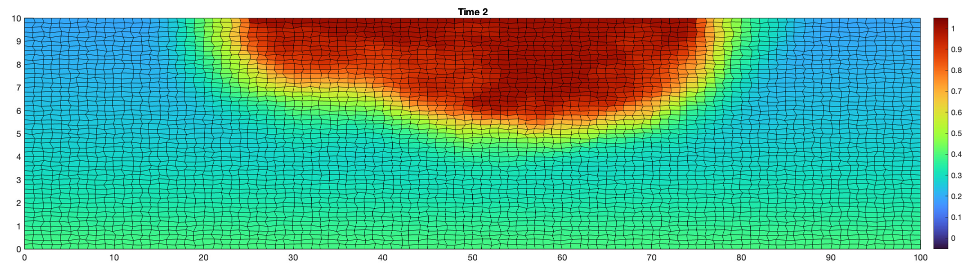

ML-WENO(3,1)

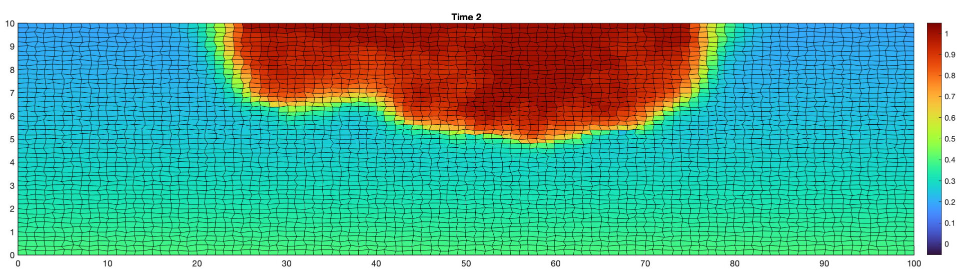

ML-WENO(3,2)

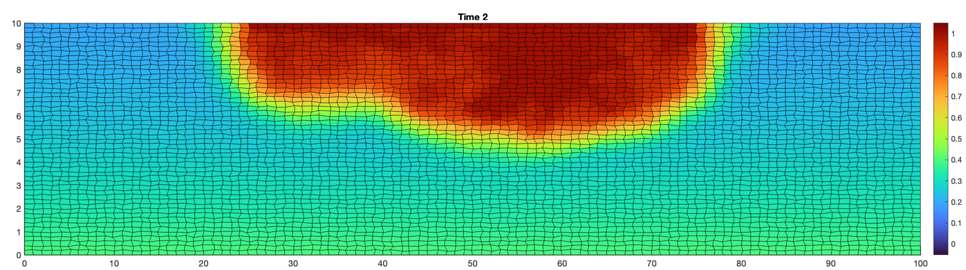

ML-WENO(3,2,1)

Day 2

Infiltration of Water at the Surface—4 days

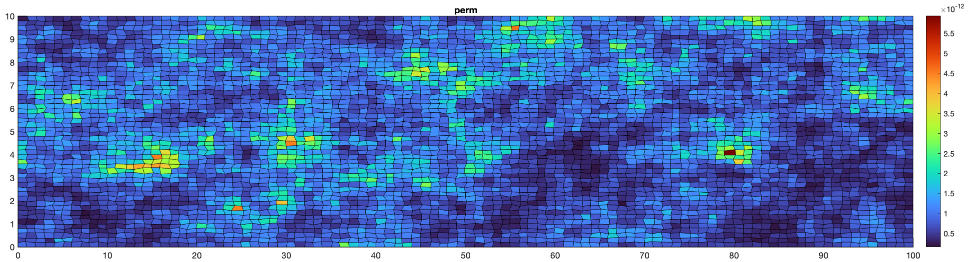

Permeability

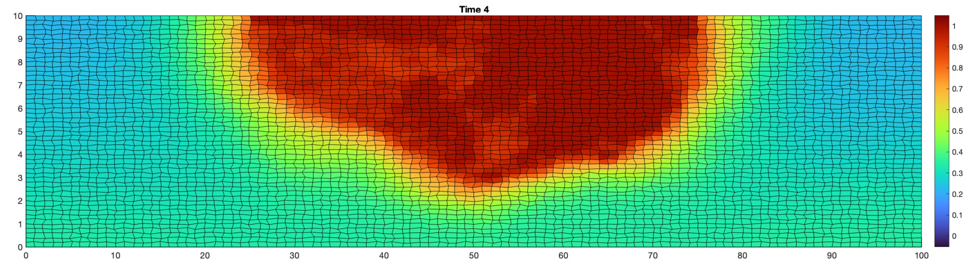

ML-WENO(1)

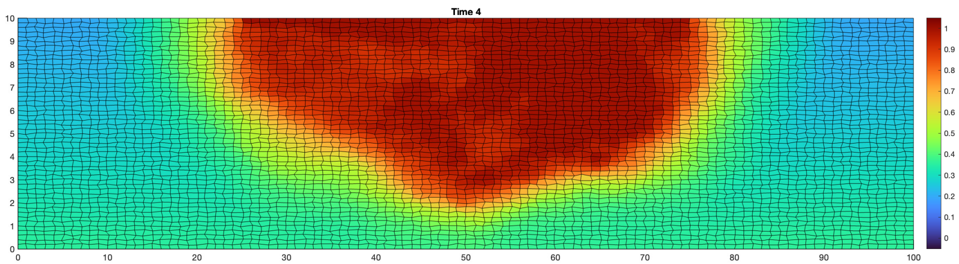

ML-WENO(2,1)

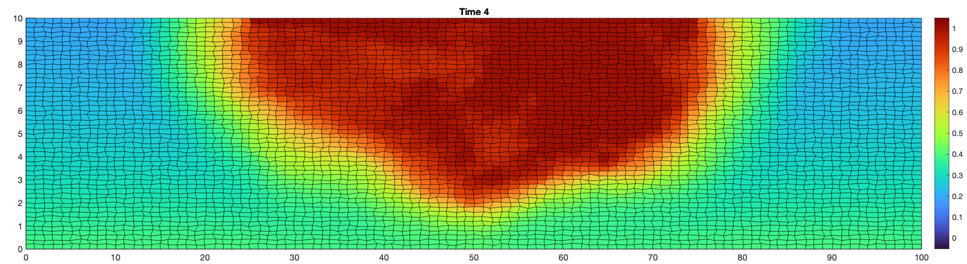

ML-WENO(3,1)

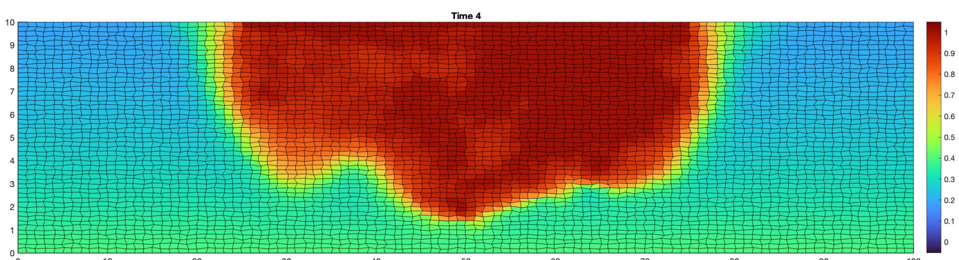

ML-WENO(3,2)

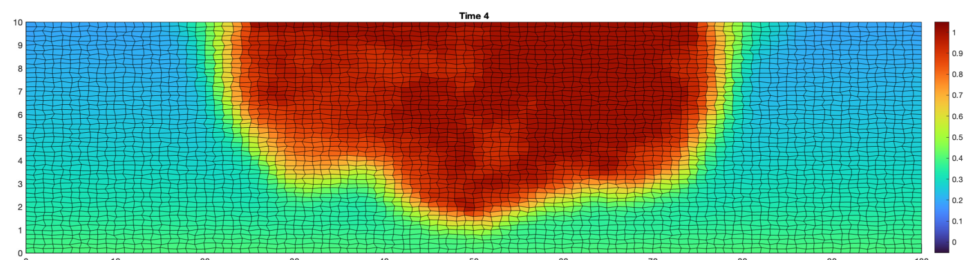

ML-WENO(3,2,1)

Day 4

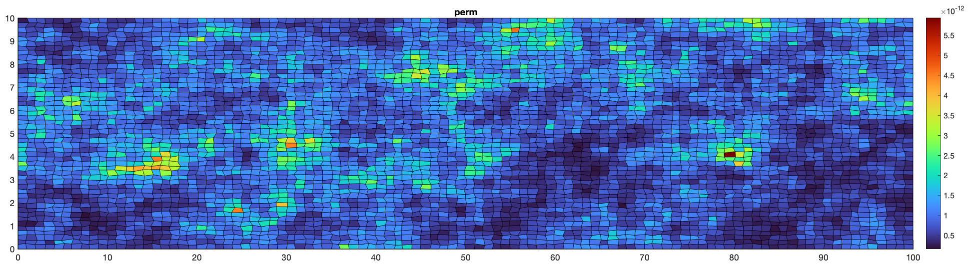

Permeability

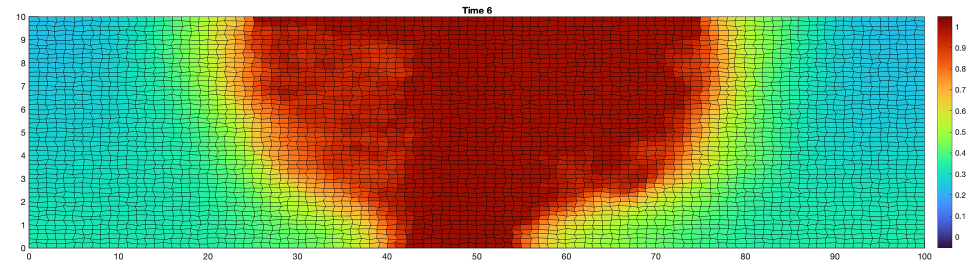

ML-WENO(1)

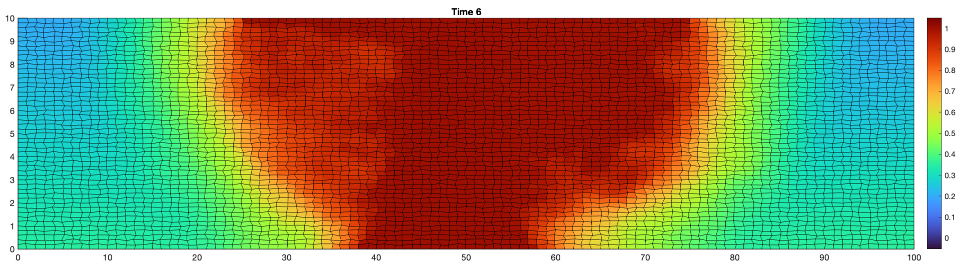

ML-WENO(2,1)

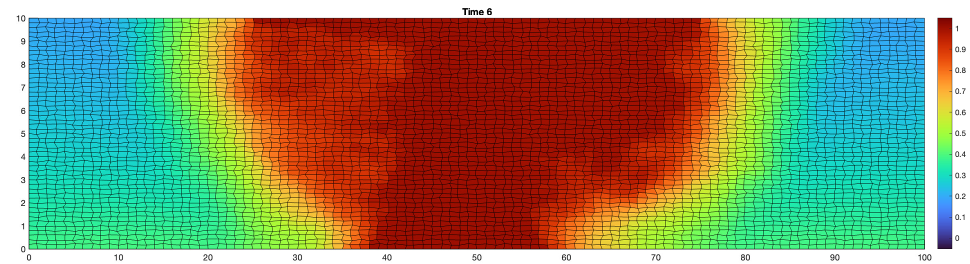

ML-WENO(3,1)

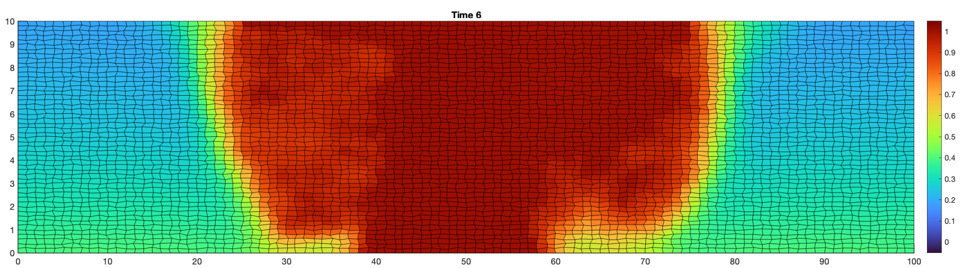

ML-WENO(3,2)

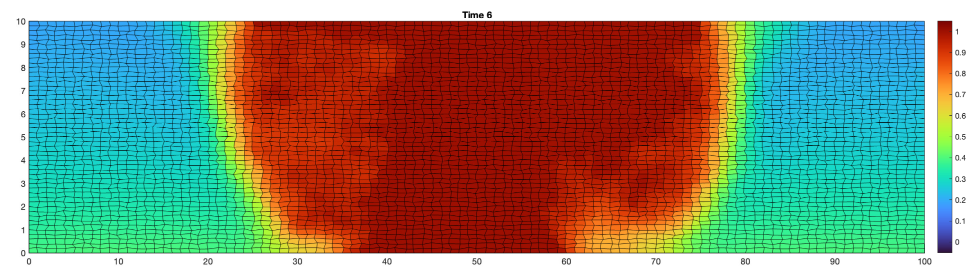

ML-WENO(3,2,1)

Day 6

IV. Summary and Conclusions

Summary and Conclusions

1. We solved **advection-diffusion** problems on **polygonal meshes** that
   - Conserve mass locally
   - Support discontinuous solutions or steep fronts
   - Are high order but (essentially) non-oscillatory
   - Use a minimal number of degrees of freedom (DoFs)

2. **Direct serendipity and mixed finite elements** on convex polygons

$$\mathcal{DS}_r = \mathbb{P}_r \oplus \mathbb{S}_r \quad \text{and} \quad \mathbf{V}_r^{r-1} = (\mathbb{P}_r)^2 \oplus \operatorname{curl} \mathbb{S}_{r+1}, \quad \mathbf{V}_r^r = \mathbf{V}_r^{r-1} \oplus \mathbf{x}\tilde{\mathbb{P}}_r$$

   - H^1 and $H(\mathrm{div})$ conforming, respectively
   - optimal order of approximation
   - Use serendipity in enriched Galerkin methods for transport
   - Use direct mixed methods for flow problems

3. **Finite volume ML-WENO** reconstruction for 2D problems

$$R(\mathbf{x}) = \sum_\ell \tilde{\omega}_\ell P_\ell(\mathbf{x})$$

   - Gives the highest order of accuracy of stencils without a shock
   - Only one degree of freedom per element
   - Use directly for advection-diffusion problems

4. Extension to **3D polytopes**
   - We have defined serendipity and mixed spaces on hexahedra
   - Finite volume methods naturally extend to 3D

References

Finite Elements

1. T. Arbogast and Chuning Wang, Direct serendipity finite elements on cuboidal hexahedra, submitted, 2024.
2. T. Arbogast and Chuning Wang, Construction of supplemental functions for direct serendipity and mixed finite elements on polygons, Mathematics 11(22):4663, 2023
3. T. Arbogast and Chuning Wang. Direct serendipity and mixed finite elements on convex polygons. *Numerical Algorithms*, 2022.
4. T. Arbogast, Zhen Tao, and Chuning Wang. Direct serendipity and mixed finite elements on convex quadrilaterals. *Numerische Mathematik*, 150:929–974, 2022.
5. T. Arbogast and Zhen Tao. A direct mixed–enriched Galerkin method on quadrilaterals for two-phase Darcy flow. *Computational Geosci.*, 23:1141–60, 2019.
6. T. Arbogast and Zhen Tao. Construction of H(div)-conforming mixed finite elements on cuboidal hexahedra. *Numer. Math.*, 142(1):1–32, 2019.
7. T. Arbogast and M. R. Correa. Two families of H(div) mixed finite elements on quadrilaterals of minimal dimension. *SIAM J. Numer. Anal.*, 54(6):3332–3356, 2016.

Finite Volumes

1. T. Arbogast, Ch.-S. Huang, and Chenyu Tian. A finite volume multilevel WENO scheme for multidimensional scalar conservation laws, Comput. Methods Appl. Mech. Engrg., 421:116818, 2024.
2. T. Arbogast, Ch.-S. Huang, and Xikai Zhao. Finite volume WENO schemes for nonlinear parabolic problems with degenerate diffusion on non-uniform meshes. *J. Comput. Phys.*, 399(108921), 2019.
3. T. Arbogast, Ch.-S. Huang, and Xikai Zhao. Accuracy of WENO and adaptive order WENO reconstructions for solving conservation laws. *SIAM J. Numer. Anal.*, 56(3):1818–1847, 2018.